

Deuterium Fractionation: the Ariadne's Thread from the Pre-collapse Phase to Meteorites and Comets today

Cecilia Ceccarelli

Université J.Fourier de Grenoble

Paola Caselli

University of Leeds

Dominique Bockelée-Morvan

Observatoire de Paris

Olivier Mousis

Université Franche-Comté and Université de Toulouse

Sandra Pizzarello

Arizona State University

Francois Robert

Muséum National d'Histoire Naturelle de Paris

Dmitry Semenov

Max Planck Institute for Astronomy, Heidelberg

The Solar System formed about 4.6 billion years ago from a condensation of matter inside a molecular cloud. Trying to reconstruct what happened is the goal of this chapter. For that, we put together our understanding of Galactic objects that will eventually form new suns and planetary systems, with our knowledge on comets, meteorites and small bodies of the Solar System today. Our specific tool is the molecular deuteration, namely the amount of deuterium with respect to hydrogen in molecules. This is the Ariadne's thread that helps us to find the way out from a labyrinth of possible histories of our Solar System. The chapter reviews the observations and theories of the deuterium fractionation in pre-stellar cores, protostars, protoplanetary disks, comets, interplanetary dust particles and meteorites and links them together trying to build up a coherent picture of the history of the Solar System formation. We emphasise the interdisciplinary nature of the chapter, which gathers together researchers from different communities with the common goal of understanding the Solar System history.

1. INTRODUCTION

The ancient Greek legend reads that Theseus volunteered to enter in the Minotaur's labyrinth to kill the monster and liberate Athens from periodically providing young women and men in sacrifice. The task was almost impossible to achieve because killing the Minotaur was not even half of the problem: getting out of the labyrinth was even more difficult. But Ariadne, the guardian of the labyrinth and daughter of the king of Crete, provided Theseus with a ball of thread, so that he could unroll it going inside and follow it back to get out of the Minotaur's labyrinth. Which he did.

Our labyrinth here is the history of the formation of the Solar System. We are deep inside the labyrinth, with the Earth and the planets formed, but we don't know how ex-

actly this happened. There are several paths that go into different directions, but what is the one that will bring us out of this labyrinth, the path Nature followed to form the Earth and the other Solar System planets and bodies?

Our story reads that once upon a time, it existed an interstellar cloud of gas and dust. Then, about 4.6 billions years ago, one cloud fragment became the Solar System. What happened to that primordial condensation? When, why and how did it happen? Answering these questions involves putting together all of the information we have on the present day Solar System bodies and micro particles. But this is not enough, and comparing that information with our understanding of the formation process of Solar-type stars in our Galaxy turns out to be indispensable too.

Our Ariadne's thread for this chapter is the deuterium

fractionation, namely the process that enriches the amount of deuterium with respect to hydrogen in molecules. Although deuterium atoms are only $\sim 1.6 \times 10^{-5}$ (Tab. 1) times as abundant as the hydrogen atoms in the Universe, its relative abundance in molecules, larger than the elemental D/H abundance in very specific situations, provides a remarkable and almost unique diagnostic tool. Analysing the deuterium fractionation in different galactic objects which will eventually form new suns, and in comets, meteorites and small bodies of the Solar System is like having in our hands a box of old photos with the imprint of memories, from the very first steps of the Solar System formation. The goal of this chapter is trying to understand the message that these photos bring, using our knowledge of the different objects and, in particular, the Ariadne's thread of the deuterium fractionation to link them together in a sequence that is the one that followed the Solar System formation.

The chapter is organised as follows. In §2, we review the mechanisms of the deuterium fractionation in the different environments and set the bases for understanding the language of the different communities involved in the study of the Solar System formation. We then briefly review the major steps of the formation process in §3. The following sections, from §4 to §9, will review in detail observations and theories of deuterium fractionation in the different objects: pre-stellar cores, protostars, protoplanetary disks, comets and meteorites. In §10, we will try to follow back the thread, unrolled in the precedent sections, to understand what happened to the Solar System, including the formation of the terrestrial oceans. We will conclude with §11.

2. THE LANGUAGE OF DEUTERIUM FRACTIONATION

2.1. Chemical processes of deuterium fractionation

Deuterium is formed at the birth of the Universe with an abundance D/H estimated to be $A_D = 1.6 \times 10^{-5}$ (Tab. 1) and destroyed in the interiors of the stars. Therefore, its abundance may vary from place to place: for example, it is lower in regions close to the Galactic Center, where the star formation is high, than in the Solar System neighborhood (*Lubowich et al., 2000*). If there were no deuterium fractionation, a species with one H-atom, like for example HCN, would have a relative abundance of D-atom over H-atom bearing molecules equal to A_D , namely $\text{DCN}/\text{HCN} = 1.6 \times 10^{-5}$. As another important example, water would have $\text{HDO}/\text{H}_2\text{O} = 2 \times A_D = 3.2 \times 10^{-5}$. Similarly, a species with two hydrogens will have a relative abundance of molecules with two D-atoms proportional to A_D^2 (e.g., $\text{D}_2\text{O}/\text{H}_2\text{O} = 2.6 \times 10^{-10}$) and so on. In practice, if there were no deuterium fractionation, the abundance of D-bearing molecules would be ridiculously low.

But in space things are special enough to make the conditions propitious for deuterium fractionation (or molecular deuteration or deuterium enrichment) to occur. This can be summarised in three basic steps, shown in Fig. 1:

1) *formation of H_3^+* : in cold (~ 10 K) molecular gas, the

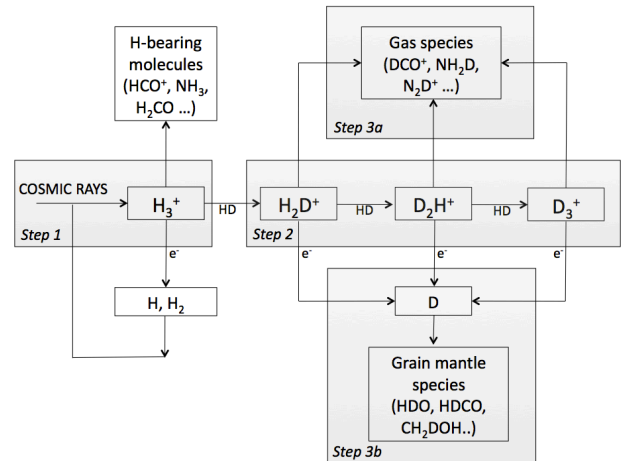


Fig. 1.— In cold (≤ 30 K) gas, deuterium fractionation occurs through three basic steps: 1) formation of H_3^+ ions from the interaction of cosmic rays with H and H_2 ; 2) formation of H_2D^+ (HD_2^+ and D_3^+) from the reaction of H_3^+ (H_2D^+ and HD_2^+) with HD; 3) formation of other D-bearing molecules from reactions with H_2D^+ (HD_2^+ and D_3^+) in the gas phase (Step 3a) and on the grain mantles (Step 3b).

fastest reactions are those involving ions, as neutral-neutral reactions have activation barriers and are generally slower. The first formed molecular ion is H_3^+ , a product of the cosmic rays ionisation of H_2 and H.

2) *Formation of H_2D^+ , D_2H^+ and D_3^+* : in cold molecular gas, H_3^+ reacts with HD, the major reservoir of D-atoms, and once every three times the D-atom is transferred from HD to H_2D^+ . The inverse reaction $\text{H}_2 + \text{H}_2\text{D}^+$ which would form HD has a (small) activation barrier so that at low temperatures $\text{H}_2\text{D}^+/\text{H}_3^+$ becomes larger than A_D . Similarly, D_2H^+ and D_3^+ are formed by reactions with HD.

3) *Formation of other D-bearing molecules*: H_2D^+ , D_2H^+ and D_3^+ react with other molecules and atoms transferring the D-atoms to all the other species. This can happen directly in the gas phase (Step 3a in Fig. 1) or on the grain mantles (Step 3b) via the D atoms created by the H_2D^+ , D_2H^+ and D_3^+ dissociative recombination with electrons. In both cases, the deuterium fractionation depends on the $\text{H}_2\text{D}^+/\text{H}_3^+$, $\text{D}_2\text{H}^+/\text{H}_3^+$ and $\text{D}_3^+/\text{H}_3^+$ abundance ratios.

Therefore, generally speaking, the basic molecule for the deuterium fractionation is H_2D^+ (and D_2H^+ and D_3^+ in extreme conditions). The cause for the enhancement of H_2D^+ with respect to H_3^+ and, consequently, deuterium fractionation is the larger mass (equivalent to a higher zero energy) of H_2D^+ with respect to H_3^+ , which causes the activation barrier in step 2. The quantity which governs whether the barrier can be overcome and, consequently, the deuterium fractionation is the temperature: the lower the temperature the larger the deuterium fractionation.

Besides, if abundant neutrals and important destruction partners of H_3^+ isotopologues, such as O and CO, deplete

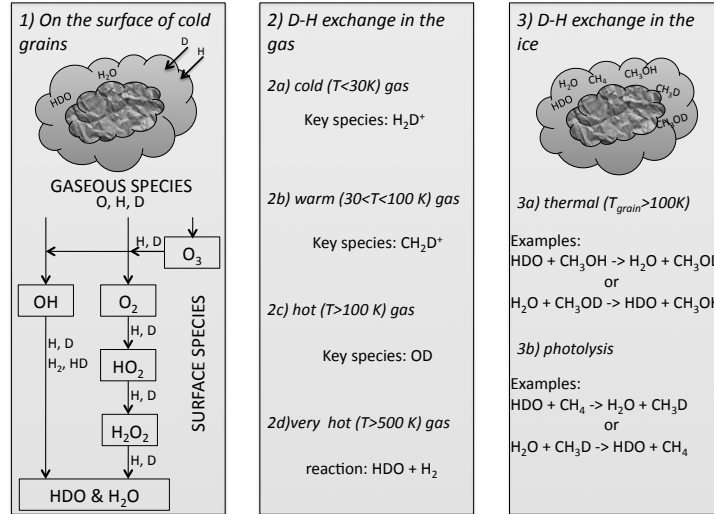


Fig. 2.— The three principal routes of water formation and deuteration. *Left panel:* gas species as atomic O, H and D land on the grain surfaces and form water through OH, O₂ and O₃ hydrogenation. *Central panel:* in the gas, water deuteration proceeds via reactions with H₂D⁺, CH₂D⁺, OD and HDO with H₂, depending on the gas temperature. *Right panel:* D and H atoms can also be exchanged between frozen species and water while they are on the grain surfaces.

from the gas-phase (for example because of the freeze-out onto dust grains in cold and dense regions; §4 and §6), the deuterium fraction further increases (Dalgarno and Lepp, 1984; Roberts et al., 2003). This is due to the fact that the destruction rates of all the H₃⁺ isotopologues drop, while the formation rate of the deuterated species increases because of the enhanced H₃⁺ abundance.

There is another factor that strongly affects the deuterium fractionation: the ortho-to-para abundance ratio of H₂ molecules. In fact, if this ratio is larger than $\sim 10^{-3}$, the internal energy of the ortho H₂ molecules (whose lowest energy level is $\sim 175\text{K}$) can be enough to overcome the H₂D⁺ + H₂ → HD + H₃⁺ barrier and limit the H₂D⁺/H₃⁺ ratio (Gerlich and Schlemmer, 2002; Flower et al., 2006; Rist et al., 2013). In general, it is believed that ortho and para H₂ are formed on the surface of dust grains with a statistical ratio of 3:1. Proton-exchange reactions then convert ortho- into para- H₂, especially at the low temperatures of dense cloud cores, where the ortho-to-para H₂ ratio is predicted to drop below 10^{-3} (Sipilä et al., 2013).

So far we have discussed the deuterium fractionation routes in cold ($T \lesssim 40 - 50\text{K}$) gas. Different routes occur in warm ($30 \lesssim T \lesssim 100\text{K}$) and hot ($100 \lesssim T \lesssim 1000\text{K}$) gas. In warm gas ($T \lesssim 70 - 80\text{K}$), the D-atoms can be transferred to molecules by CH₂D⁺, whose activation barrier of the reaction with H₂ is larger than that of H₂D⁺ (Roberts and Millar, 2000). At even higher temperatures, OD transfers D-atoms from HD to water molecules (Thi et al., 2010b). In these last two cases, CH₂D⁺ and OD

play the role of H₂D⁺ at lower temperatures. At $\gtrsim 500\text{K}$ water can directly exchange D and H atoms with H₂ (Geiss and Reeves, 1981; Lécluse and Robert, 1994).

Finally, some molecules, notably water, are synthesised on the surfaces of interstellar and interplanetary grains by addition and/or substitution of H and D atoms (§2.2). In this case, the deuterium fractionation depends on the D/H ratio of the atomic gas. As discussed previously in this section, the enhanced abundance of H₂D⁺ (D₂H⁺ and D₃⁺) also implies an increased atomic D/H ratio in the gas (Step 3b in Fig. 1), as deuterium atoms are formed upon dissociative recombination of the H₃⁺ deuterated isotopologues, whereas H atoms maintain an about constant density of $\gtrsim 1\text{cm}^{-3}$, determined by the balance between surface formation and cosmic-ray dissociation of H₂ molecules (Li and Goldsmith, 2003).

2.2. Deuterium fractionation of water

Given the particular role of deuterated water in understanding the Solar System history, we summarize the three major processes (reported in the literature) that cause the water deuteration. They are schematically shown in Fig. 2. *1) Formation and deuteration on the surfaces of cold grains:* in cold molecular clouds and star forming regions, water is mostly formed by H and D atoms addition to O, O₂ and O₃ on the grain surfaces, as demonstrated by several laboratory experiments (Hiraoka et al., 1998; Dulieu et al., 2010; Oba et al., 2012). In this case, therefore, the key parameter governing the water deuteration is the atomic D/H

Acronym	Definition				
<i>aa</i>	Amino acids.				
A_V	Visual extinction, measured in magnitudes (mag), proportional to the H nuclei column density in the line of sight.				
ALMA	Atacama Large Millimeter Array.				
CSO	Caltech Submillimeter Observatory.				
HSO	Herschel Space Observatory.				
JCMT	James Clerk Maxwell Telescope.				
IOM	Insoluble Organic Matter.				
ISM	Inter-Stellar Medium.				
NOEMA	Northern Extended Millimeter Array.				
PSN	Proto Solar Nebula.				
SOC	Soluble Organic Compounds (same as SOM).				
SOM	Soluble Organic Matter (same as SOC).				
VLT	Very Large Telescope.				
Astrophysical key objects mentioned in the chapter					
PSC	Pre-stellar Cores: dense and cold condensations, they are the first step of solar type star formation.				
Class 0	Class 0 sources: youngest known solar type protostars.				
Hot corino	The warm and dense inner regions of the envelopes of Class 0 protostars.				
PPD	Proto-Planetary Disks: disks of material surrounding young protostars.				
Origin of the Solar System bodies mentioned in the chapter					
JFC	Jupiter-family comets: ecliptic short-period comets, whose reservoir is the Kuiper belt. Probably formed in the trans-Neptunian region.				
OCC	Oort-cloud comets: long-period comets, whose reservoir is the Oort cloud. Probably formed in the Uranus-Neptune region, with some contribution from the Jupiter-Saturn region.				
CCs	Carbonaceous Chondrites: the most primitive meteorites, mostly coming from the main belt (2-4 AU).				
IDPs	Interplanetary Dust Particles: At least 50% are fragments of comets, the rest fragments of main belt asteroids.				
Measure of molecular deuteration:					
1) In geochemical and biochemical studies, the molecular deuteration is measured by the deuterium enrichment in a sample compared to that of a chosen standard value, in ‰ with respect to the standard ratio. For deuterium: $\delta D = \frac{D/H_{sample} - D/H_{VSMOW}}{D/H_{VSMOW}} \times 10^3$					
2) In astrochemical studies, the molecular deuteration is measured by the heavy/light isotope abundance.					
3) In the PSN models, the molecular deuteration is given by the enrichment factor f , defined as the ratio between the molecule D/H and the PSN D/H.					
Acronym	Definition	D/H	δD	f	references
A_D	Cosmic elemental deuterium abundance	1.6×10^{-5}	-900	0.8	a
PSN D/H	Deuterium abundance in the PSN	2.1×10^{-5}	-860	1.0	b
VSMOW	Vienna Standard Mean Ocean Water (refers to evaporated ocean waters)	1.5×10^{-4}	0	7.1	c

Table 1: Definitions of symbols and terms used in the Chapter. References: a: *Linsky (2007)*. b: *Geiss and Gloeckler (1998)*. c: *Lécuyer et al. (1998)*.

FROM A DIFFUSE CLOUD TO A SUN-LIKE + PLANETARY SYSTEM THE DEUTERIUM FRACTIONATION HISTORY

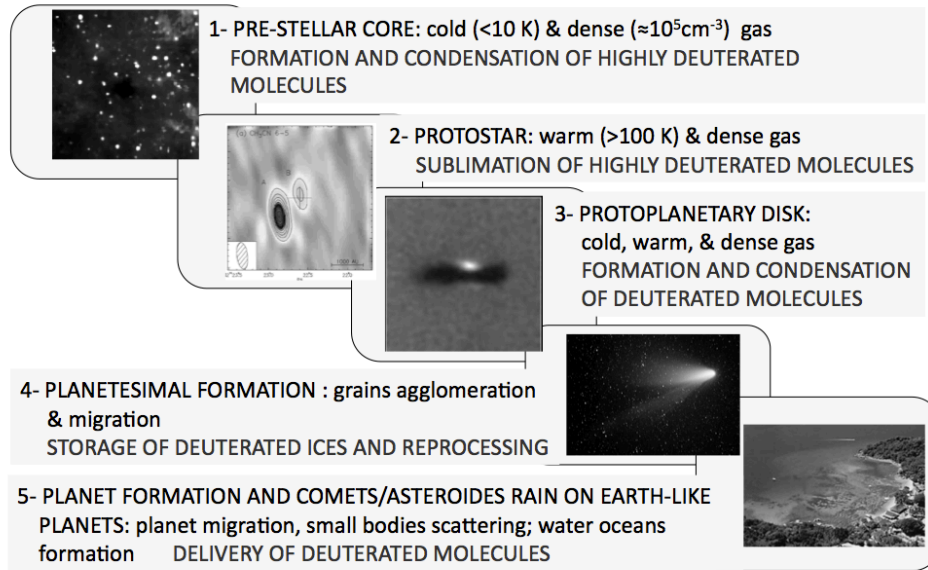


Fig. 3.— Schematic summary of the different phases that likely gave birth to the Solar System, with highlighted the main deuterium processes (adapted from Caselli & Ceccarelli 2012).

ratio in the gas, which depends on the $\text{H}_2\text{D}^+/\text{H}_3^+$ ratio as discussed in the previous section.

2) *Hydrogen-Deuterium exchange in the gas phase*: as for any other molecule, D-atoms can be transferred from H_2D^+ (D_2H^+ and D_3^+) to H_2O in cold gas (Sec. 2.1), and more efficiently through the $\text{HD} + \text{OH}^+ \rightarrow \text{HDO} + \text{H}$ and $\text{HD} + \text{OH}_2^+ \rightarrow \text{HDO} + \text{H}_2$ reactions. In warm gas, it is in principle possible to have direct exchange between HD and H_2O to form HDO (Geiss and Reeves, 1981; Lécluse and Robert, 1994). However, being a neutral-neutral reaction, it possesses an activation barrier (Richet et al., 1977), which makes this route very slow at $T \lesssim 500$ K. On the contrary, for temperatures high enough (≥ 100 K), the $\text{OH} + \text{HD}$ and $\text{OD} + \text{H}_2$ reactions can form HDO. Based on modelling, Thi et al. (2010b) demonstrated that the $\text{HD} + \text{O} \rightarrow \text{OD} + \text{H}$ followed by the $\text{OD} + \text{H}_2 \rightarrow \text{HDO} + \text{H}$ reaction is indeed a major route for the HDO formation in warm gas.

3) *Isotopic exchange between solid H_2O and HDO with other solid species*: laboratory experiments have shown that D and H atoms can be exchanged between water ice and other molecules trapped in the ice, like for example CH_3OH (Ratajczak et al., 2009; Gálvez et al., 2011). Very likely, the exchange occurs during the ice sublimation phase, with the re-organisation of the crystal. Similarly, H-D exchange in ice can be promoted by photolysis (Weber et al., 2009). Note that this mechanism not only can alter the $\text{HDO}/\text{H}_2\text{O}$ abundance ratio in the ice, but also it can pass D-atoms to organic matter trapped in the ice, enriching it of deuterium.

2.3. Towards a common language

This chapter has the ambition to bring together researchers from different communities. One of the disadvantages, which we aim to overcome here, is that these different communities do not always speak the same language. Table 1 is a sort of dictionary which will help the reader to translate the chapter in her/his own language. In addition, several acronyms used throughout this chapter are also listed in the table. With this, we are ready now to start our voyage through the different objects.

3. A BRIEF HISTORY OF THE SOLAR SYSTEM FORMATION

According to the widely accepted scenario, the five major phases of solar type star formation are (Fig. 3):

- 1: **Pre-stellar cores.** These are the starting point of Solar-type star formation. In these "small clouds" with evidence of contraction motions, contrarily to starless cores, matter slowly accumulates toward the center, causing the increase of the density while the temperature is kept low ($\lesssim 10$ K). Atoms and molecules in the gas-phase freeze-out onto the cold surfaces of the sub-micron dust grains, forming the so called icy grain mantles. This is the moment when the deuterium fractionation is most effective: the frozen molecules, including water, acquire a high deuterium fraction.

- 2: **Protostars.** The collapse starts, the gravitational energy is converted into radiation and the envelope around the central object, the future star, warms up. When and where the temperature reaches the mantle sublimation temperature ($\sim 100\text{--}120$ K), in the so-called hot corinos, the molecules in the mantles are injected into the gas-phase, where they are observed via their rotational lines. Complex organic molecules, precursors of prebiotic species, are also detected at this stage.
- 3: **Protoplanetary disks.** The envelope dissipates with time and eventually only a circumstellar, protoplanetary disk remains. In the hot regions, close to the central object or the disk surface, some molecules, notably water, can be D-enriched via neutral-neutral reactions. In the cold regions, in the midplane, where the vast majority of matter resides, the molecules formed in the protostellar phase freeze-out again onto the grain mantles, where part of the ice from the pre-stellar phase may still be present. The deuterium fractionation process becomes again important.
- 4: **Planetesimals formation.** The process of "conservation and heritage" begins. The sub-micron dust grains coagulate into larger rocks, called planetesimals, the seeds of the future planets, comets and asteroids. Some of the icy grain mantles are likely preserved while the grains glue together. At least part of the previous chemical history may be conserved in the building blocks of the forming planetary system rocky bodies and eventually passed as an heritage to the planets. However, migration and diffusion may scramble the original distribution of the D-enriched material.
- 5: **Planet formation.** The last phase of rocky planet formation is characterized by giant impacts between planet embryos, which, in the case of the Solar System, resulted in the formation of the Moon and Earth. Giant planets may migrate, inducing a scattering of the small bodies all over the protoplanetary disk. Oceans are formed on the young Earth and, maybe in other rocky planets. The leftovers of the process become comets and asteroids. In the Solar System, their fragments continuously rain on Earth releasing the heritage stored in the primitive D-enriched ices. Life takes over sometime around 2 billion years after the Earth and Moon formation (Czaja, 2010).

In the rest of the chapter, we will discuss each of these steps, the measured deuterium fractionation and the processes responsible for that.

4. THE PRE-STELLAR CORE PHASE

4.1. The structure of pre-stellar cores

Stars form within fragments of molecular clouds, the so-called dense cores (Benson and Myers, 1989), produced by

the combined action of gravity, magnetic fields and turbulence (McKee and Ostriker, 2007). Some of the starless dense cores can be transient entities and diffuse back into the parent cloud, while others (the pre-stellar cores) will dynamically evolve until the formation of one or more planetary systems. It is therefore important to gather kinematics information to identify pre-stellar cores, which represent the initial conditions in the process of star and planet formation. Their structure and physical characteristics depend on the density and temperature of the surrounding cloud, i.e. on the external pressure (Tan et al., this volume). The well-studied pre-stellar cores in nearby molecular clouds have sizes of $\simeq 10,000$ AU, similar to the Oort cloud, masses of a few Solar masses and visual extinctions $\gtrsim 50$ mag. They are centrally concentrated (Ward-Thompson et al., 1999), with central densities larger than 10^5 H_2 cm^{-3} (Bacmann et al., 2003; Crapsi et al., 2005; Keto and Caselli, 2008), central temperatures close to 7 K (Crapsi et al., 2007; Pagani et al., 2007) and with evidence of subsonic gravitational contraction (Keto and Caselli, 2010) as well as gas accretion from the surrounding cloud (Lee and Myers, 2011). The ESA Herschel satellite has detected water vapour for the first time toward a pre-stellar core and unveiled contraction motions in the central $\simeq 1,000$ AU (Caselli et al., 2012): large amounts of water (a few Jupiter masses, mainly in ice form) are transported toward the future Solar-type star and its potential planetary system.

A schematic summary of the main chemical and physical characteristics of pre-stellar cores is shown in Figure 4. The upper left panel shows one of the best studied objects: L1544 in the Taurus Molecular Cloud Complex, 140 pc away. The largest white contour roughly indicates the size of the dense core and the outer edge represents the transition region between L1544 and the surrounding molecular cloud, where the extinction drops below $\simeq 4$ mag and photochemistry becomes important. This is where water ice copiously form on the surface of dust grains (Whittet et al., 2007; Hollenbach et al., 2009) and low-levels of water deuteration are taking place (Cazaux et al., 2011; Taquet et al., 2012a). Within the *dark-cloud zone*, where the carbon is mostly locked in CO, gas-phase chemistry is regulated by ion-molecule reactions (Fig. 4, top right panel).

Within the central $\simeq 7,000$ AU, the volume density becomes higher than a few $\times 10^4$ cm^{-3} (see bottom panel) and the freeze-out timescale ($\simeq 10^9/n_{\text{H}}$ yr) becomes shorter than a few $\times 10^4$ yr. This is the *deuteration zone*, where the freeze-out of abundant neutrals such as CO and O, the main destruction partners of H_3^+ isotopologues, favour the formation of deuterated molecules (see Sect. 2.1). Deuteration is one of the main chemical process at work, making deuterated species the best tools to study the physical structure and dynamics of the earliest phases of star formation.

4.2. Deuterium fractionation

Pre-stellar cores chemically stand out among other starless dense cores, as they show the largest deuterium frac-

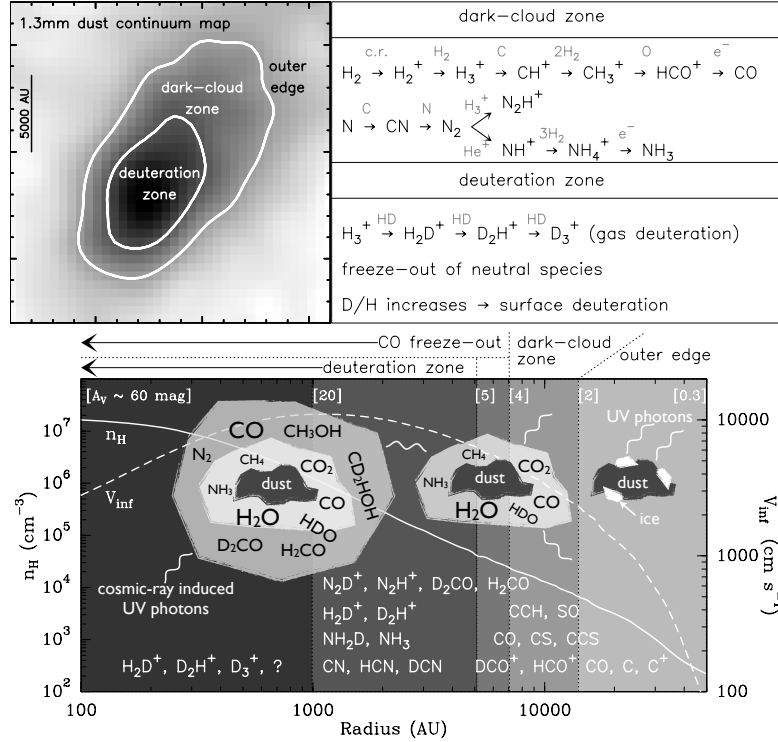


Fig. 4.— Schematic summary of the main physical and chemical characteristics of a pre-stellar core. *Upper left panel.* The grey scale is the 1.2 mm dust continuum emission of L1544, the prototypical pre-stellar core (data from *Ward-Thompson et al., 1999*). White contours mark the transition from the outer edge to the dense core and the deuteration zone, where CO is highly frozen onto dust grains. *Upper right panel.* Main chemical processes in the dark-cloud zone and the deuteration zone. Grey symbols above the arrows are the reaction partners and the arrow indicates the reaction direction. *Bottom panel.* Radial slice of L1544, indicating the number density (n_{H}), infall velocity (V_{inf}) profiles, the visual extinction A_V , the main molecular diagnostic tools in the various zones and a rough summary of dust grain evolution within the pre-stellar core (see also *Caselli and Ceccarelli, 2012*).

tions ($>10\%$; *Bacmann et al., 2003; Crapsi et al., 2005; Pagani et al., 2007*) and CO depletions ($>90\%$ of CO molecules are frozen onto dust grain surfaces; *Caselli et al., 1999; Bacmann et al., 2002*). The largest D-fractions have been observed in N_2H^+ ($\text{N}_2\text{D}^+/\text{N}_2\text{H}^+ \simeq 0.1\text{--}0.7$; *Crapsi et al., 2005; Pagani et al., 2007*), ammonia ($\text{NH}_2\text{D}/\text{NH}_3 \simeq 0.1\text{--}0.4$; *Shah and Wootten, 2001; Crapsi et al., 2007*), and formaldehyde ($\text{D}_2\text{CO}/\text{H}_2\text{CO} \simeq 0.01\text{--}0.1$; *Bacmann et al., 2003*). HCN, HNC and HCO^+ show somewhat lower deuterations (between 0.01 and 0.1; *Turner, 2001; Hirota et al., 2003; Butner et al., 1995; Caselli et al., 2002*). *Spezzano et al. (2013)* recently detected doubly deuterated cyclopropenylidene ($c\text{-C}_3\text{D}_2$), finding a $c\text{-C}_3\text{D}_2/c\text{-C}_3\text{H}_2$ abundance ratio of about 0.02. Unfortunately, no measurement of water deuteration is available yet.

Pre-stellar cores are the strongest emitters of the ground state rotational transition of ortho- H_2D^+ (*Caselli et al., 2003*) and the only objects where para- D_2H^+ has been detected (*Vastel et al., 2004; Parise et al., 2011*). It is interesting to note that the strength of the ortho- H_2D^+ line does not correlate with the amount of deuterium fraction found in other molecules. This is probably due to variations of the H_2D^+ ortho-to-para ratio in different environments (*Caselli*

et al., 2008), an important clue in the investigation of how external conditions affect the chemical and physical properties of pre-stellar cores (see also *Friesen et al., 2013*).

4.3. Origin of deuterium fractionation

Pre-stellar cores are "deuterium fractionation factories". The reason for this is twofold: firstly, they are very cold (with typical gas and dust temperatures between 7 and 13 K). This implies a one-way direction of the reaction $\text{H}_3^+ + \text{HD} \rightarrow \text{H}_2\text{D}^+ + \text{H}_2$, the starting point of the whole process of molecular deuteration (see Fig.1, step 2 and 3a). Secondly, a large fraction of neutral heavy species such as CO and O freeze-out onto dust grains. As mentioned in §2.1, the disappearance of neutrals from the gas phase implies less destruction events for H_3^+ and its deuterated forms, with consequent increase of not just H_2D^+ but also D_2H^+ and D_3^+ (*Dalgarno and Lepp, 1984; Roberts et al., 2003; Walmley et al., 2004*). This simple combination of low temperatures and the tendency for molecules to stick on icy mantles on top of dust grains, can easily explain the observed deuterium fraction measured in pre-stellar cores (see also *Roueff et al., 2005*).

The case of formaldehyde (H_2CO) deuteration requires

an extra note, as not all the data can be explained by gas-phase models including freeze-out. As discussed in *Bacmann et al.* (2003), another source of deuteration is needed. A promising mechanism is the chemical processing of icy mantles (surface chemistry), coupled with partial desorption of surface molecules upon formation (*Garrod et al.*, 2006). In particular, once CO freezes out onto the surface of dust grains, it can either be stored in the ice mantles, or be "attacked" by reactive elements, in particular atomic hydrogen. In the latter case, CO is first transformed into HCO, then formaldehyde and eventually into methanol (CH₃OH). In pre-stellar cores, deuterium atoms are also abundant because of the dissociative recombination of the abundant H₂D⁺, D₂H⁺ and possibly D₃⁺ (see Fig.1, step 3b). Chemical models predict D/H between 0.3 and 0.9 in the inner zones of pre-stellar cores with large CO freeze-out (*Roberts et al.*, 2003; *Taquet et al.*, 2012a), implying a large deuteration of formaldehyde and methanol on the surface of dust grains (see dust grain cartoons overlaid on the bottom panel of Fig.4). Thus, the measured large deuteration of gas-phase formaldehyde in pre-stellar cores (and possibly methanol, although this still awaits for observational evidence) can be better understood with the contribution of surface chemistry, as a fraction of surface molecules can desorb upon formation (thanks to their formation energy).

5. THE PROTOSTAR PHASE

5.1. The structure of the Class 0 protostars

Class 0 sources are the youngest protostars. Their luminosity is powered by the gravitational energy, namely the material falling towards the central object, accreting it at a rate of $\lesssim 10^{-5} M_{\odot}/\text{yr}$. They last for a short period, $\sim 10^5$ yr (*Evans et al.*, 2009) (see also Dunham et al. this volume). The central object, the future star, is totally obscured by the collapsing envelope, whose sizes are $\sim 10^4$ AU, as the pre-stellar cores (§4). It is not clear whether a disk exists at this stage (*Maury et al.*, 2010), as the original magnetic field frozen on the infalling matter tends to inhibit its formation (*Z.-Y. Li et al.*, this volume). On the contrary, powerful outflows of supersonic matter are one of the notable characteristics of these objects (*Frank et al.*, this volume).

In Class 0 protostars, the density of the envelope increases with decreasing distance from the centre ($n \propto r^{-3/2}$), as well as the temperature (*Ceccarelli et al.*, 1996; *Jørgensen et al.*, 2002). From a chemical point of view, the envelope is approximatively divided in two regions, delimited by the ice sublimation temperature (100–120 K): a cold outer envelope, where molecules are more or less frozen onto the grain mantles, and an inner envelope, called hot corino, where the mantles, built up during the pre-stellar core phase (§4), sublimate (*Ceccarelli et al.*, 2000) (see *Caselli and Ceccarelli*, 2012, for a more accurate description of the Class 0 protostars). This transition occurs at distances from the center between 10 and 100 AU, depending on the source luminosity (*Maret et al.*, 2004, 2005). Relevant to this chapter, in the hot corinos, the species formed

at the pre-stellar core epoch are injected into the gas phase, bringing memory of their origin. For different reasons, the outer envelope and the hot corino have molecules highly enriched in deuterium: in the first case because of the low temperatures and CO depletion (§2.1 and §4), in the second case because of the inheritance of the pre-stellar ices.

5.2. Deuterium fractionation

Class 0 protostars are the objects where the highest deuterium fractionation has been detected so far and the first where the extreme deuteration, called in literature super-deuteration, has been discovered (*Ceccarelli et al.*, 1998, 2007): doubly and even triply deuterated forms with D/H enhancements with respect to the elemental D/H abundance (Tab. 1) of up to 13 orders of magnitude.

The first and the vast majority of measurements were obtained with single dish observations, so that they cannot disentangle the outer envelope and the hot corino, if not indirectly by modelling the line emission in some cases (*Coutens et al.*, 2012, 2013a). The following species with more than two atoms of deuterium have been detected (see *Ceccarelli et al.* (2007) for a list of singly deuterated species): formaldehyde (D₂CO: *Ceccarelli et al.*, 1998; *Parise et al.*, 2006), methanol (CHD₂OH and CD₃OH: *Parise et al.*, 2002, 2004, 2006), ammonia (NHD₂ and ND₃: *Loinard et al.*, 2001; *van der Tak et al.*, 2002; *Lis et al.*, 2002), hydrogen sulphide (D₂S: *Vastel et al.*, 2004), thioformaldehyde (D₂CS: *Marcelino et al.*, 2005) and water (D₂O: *Butner et al.*, 2007; *Vastel et al.*, 2010). In a few cases, interferometric observations provided us with measurements of water deuterium fractionation in the hot corinos (*Codella et al.*, 2010; *Persson et al.*, 2012; *Taquet et al.*, 2013a). Finally, recent observations have detected deuterated species in molecular outflows (*Codella et al.*, 2010, 2012). The situation is graphically summarized in Fig. 5.

We note that the methanol deuteration depends on the bond energy of the functional group which the hydrogen is located. In fact, the abundance ratio CH₂DOH/CH₃OD is larger than ~ 20 (*Parise et al.*, 2006; *Ratajczak et al.*, 2011), whereas it should be 3 if the D-atoms were statistically distributed. To explain this, it has been invoked that CH₃OD could be selectively destroyed in the gas-phase (*Charnley et al.*, 1997), that H–D exchange reactions in solid state could contribute to reduce CH₃OD (*Nagaoka et al.*, 2005), or, finally, that the CH₃OD under abundance is due to D–H exchange with water in the solid state (*Ratajczak et al.*, 2009, 2011). The reason for this over-deuteration of the methyl group with respect to the hydroxyl group may help to understand the origin of the deuterium fractionation in the different functional groups of the Insoluble Organic Matter (§8; see Fig. 11). This point will be discussed further in §10.

The measure of the abundance of doubly deuterated species can also help to understand the formation/destruction routes of the species. Fig. 6 shows the D/D₂ abundance ratio of the molecules in Fig. 5. For species forming on the

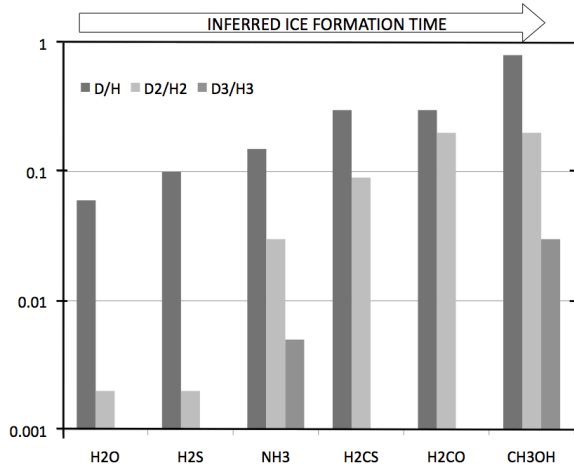


Fig. 5.— Measured deuteration ratios of singly, doubly and triply deuterated isotopologues (adapted from *Caselli and Ceccarelli*, 2012). Modelling the formation of H_2O , H_2CO and CH_3OH (*Cazaux et al.*, 2011; *Taquet et al.*, 2013b) suggests that the increasing deuteration reflects the formation time of the species on the ices. References: H_2O : *Liu et al.* (2011), *Coutens et al.* (2012), *Taquet et al.* (2013a), *Butner et al.* (2007), *Vastel et al.* (2010); H_2S : *Vastel et al.* (2003); NH_3 : *Loinard et al.* (2001), *van der Tak et al.* (2002); H_2CS : *Marcelino et al.* (2005); H_2CO : *Ceccarelli et al.* (1998); *Parise et al.* (2006); CH_3OH : *Parise et al.* (2002, 2004, 2006).

grain surfaces, if the D atoms were purely statistically distributed, namely just proportional to the D/H ratio, then it would hold: $\text{D-species}/\text{D}_2\text{-species} = 4 (\text{D-species}/\text{H-species})^{-1}$. As shown in Fig. 6, this is not the case for H_2O , NH_3 , H_2CS and H_2CO . A plausible explanation is that the D and D_2 -bearing forms of these species are formed at different times on the grain surfaces: the larger the deuterium fraction the younger the species (see §5.3).

In the context of this chapter, the deuteration of water deserves particular attention. Being water very difficult to observe with ground based telescopes (van Dishoeck et al., this volume), measurements of $\text{HDO}/\text{H}_2\text{O}$ exist only towards four Class 0 sources, and they are, unfortunately, even in disagreement. Table 2 summarizes the situation. With the ALMA facility it will be possible to settle the issue in a near future. Nonetheless, one thing is already clear from those measurements: the deuteration of water is smaller than that of the other molecules. This is confirmed also by the upper limits on the $\text{HDO}/\text{H}_2\text{O}$ in the solid phase: $\lesssim 1\%$ (*Dartois et al.*, 2003; *Parise et al.*, 2003).

5.3. Origin of the deuterium fractionation

As discussed in §2.1 and §4, the key elements for a large deuterium fractionation are a cold and CO depleted gas. The large D-enrichment observed in Class 0 sources, and especially in the hot corinos is, therefore, necessarily inherited from the pre-stellar core phase. The short lifetimes estimated for the Class 0 sources support that statement. The different D fractionation then tells us of the past

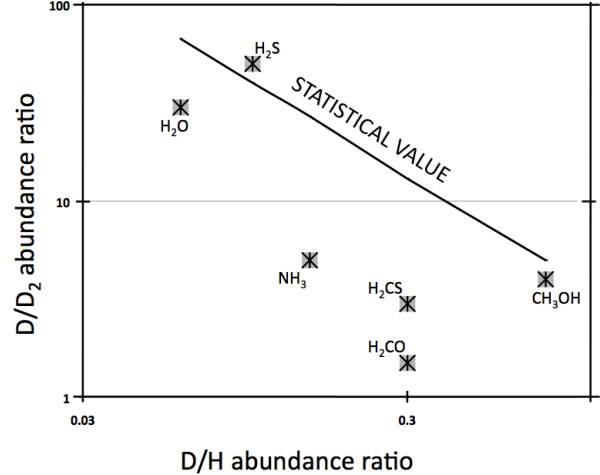


Fig. 6.— Measured ratios of singly to doubly deuterated isotopologues of the species marked in the plot. The line shows the statistical value if the D atoms were statistically distributed in the molecules formed on the grain surfaces. References as in Fig. 5. Adapted from *Caselli and Ceccarelli* (2012).

Source	$\text{HDO}/\text{H}_2\text{O}$ (10^{-3})	Note	Ref.
IRAS16293-2423	3–15	out	1
	4–51	hc	1
	0.7–1.2	hc	2
NGC1333-IRAS2A	9–180	out	3
	~ 1	hc	3, 4
NGC1333-IRAS4A	3–80	hc	5
	5–30	hc	5
NGC1333-IRAS4B	≤ 0.6	hc	6

Table 2: Measurement of the $\text{HDO}/\text{H}_2\text{O}$ ratio in Class 0 sources. In the third column we report whether the measure refers to the outer envelope (out) or the hot corino (hc). References: 1: *Coutens et al.* (2012, 2013b). 2: *Persson et al.* (2012). 3: *Liu et al.* (2011). 4: *Visser et al.* (2013). 5: *Taquet et al.* (2013a). 6: *Jørgensen and van Dishoeck* (2010).

history of the Class 0 sources. Following §4, it is very likely that water, formaldehyde and methanol were formed on the grain surface at that epoch, by hydrogenation of O and CO. The O hydrogenation leading to water occurs first, during the molecular cloud phase, and, once formed, water remains frozen on the grains (*Hollenbach et al.*, 2009). CO hydrogenation leading to H_2CO and, subsequently, to CH_3OH occurs later, in the pre-stellar core phase (*Taquet et al.*, 2012b). Consequently, the water D enrichment is lower than that of H_2CO and CH_3OH . In other words, the increasing of the D-enrichment, linked to the $\text{H}_2\text{D}^+/\text{H}_3^+$ ratio (§2.1) corresponds to a later formation of the molecule. Models by *Cazaux et al.* (2011) and *Taquet et al.* (2012a, 2013b) provide quantitative estimates in excellent agreement with the observed values. The same explanation applied to Fig. 6, tells us that H_2CO was synthesised in a large interval of time, so that the singly and doubly deuter-

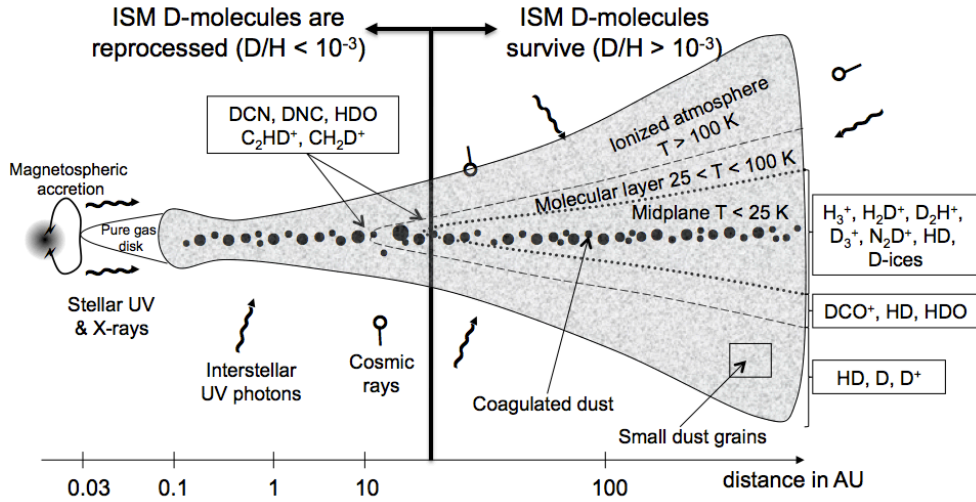


Fig. 7.— Schematic vertical cut through a protoplanetary disk around a Sun-like T Tauri star. From the chemical point of view, the disk can be divided into 3 layers: (1) the cold midplane dominated by ices and grain surface processes, (2) the warmer molecular layer with active gas-grain processes, where many gaseous molecules concentrate, and (3) the hot irradiated atmosphere dominated by photochemistry and populated by ions and small molecules.

ated forms did not inherit the same D/H atomic ratio. On the contrary, CH_3OH was formed on a short time interval. Again, this agrees with model predictions

6. THE PROTOPLANETARY DISK PHASE

6.1. The structure of protoplanetary disks

The protostellar phase has a short life time (~ 0.5 Myr), during which the powerful outflows disperse the surrounding envelope, reducing the infall of material from the envelope onto the young disks and the accretion of material from the disk to the protostar. The central few hundred astronomical units are eventually revealed and the “classical” protoplanetary disk (PPD) phase starts. This is the last, dynamically active stage, lasting several Myr, when the remaining $\sim 0.001 - 0.1 M_\odot$ of gas and dust is accreted onto the newly formed central star and assembled into a planetary system.

A summary of the physical and chemical structure of a protoplanetary disk of a Proto Solar Nebula (PSN) analogue (a T Tauri star) is sketched in Fig.7 (a more detailed description can be found in Dutrey et al. and Testi et al., this volume; (see also Caselli and Ceccarelli, 2012; Henning and Semenov, 2013, and references therein). Starting from the location of the accreting protostar, undergoing magnetospheric accretion and emitting UV photons and X-rays, we note that the first fraction astronomical unit is mainly deprived of dust, because of the large temperatures, above the dust melting point ($\simeq 1500$ K). The dusty disk starts at around 0.1 AU with an inner wall, puffed-up by the high temperature (Dullemond et al., 2002). The rest of the disk, up to a few hundred AU, can be approximately divided in three layers: (1) the ionised atmosphere, where the chem-

istry is dominated by photodissociation due to stellar and interstellar UV photons as well as stellar X-rays (Thi et al., 2010a; Aresu et al., 2012). (2) A warm molecular layer, where molecules survive but photochemistry still plays an important role (Dominik et al., 2005; Henning et al., 2010). (3) The cooler zones around the midplane, where the temperature drops to values close to those measured in pre-stellar cores (§4). The densities (up to $\sim 10^{11} \text{ cm}^{-3}$) are significantly higher than those of pre-stellar cores (up to a few times 10^7 cm^{-3}), so that dust coagulation, freeze-out and deuterium fractionation are expected to proceed faster (Ceccarelli and Dominik, 2005). The temperature increases vertically, away from the midplane, and radially, toward the central object. For a T Tauri star as that in Fig. 7, the inner region ($1 < \text{radius} < 30$ AU) has temperatures between $\simeq 30$ and 150 K, while lower temperatures are found in the midplane at $\gtrsim 30$ AU.

The sketch in Fig. 7 is of course only a rough snapshot. During the several Myr of its life time, the disk thermal and density structure, X-ray/UV radiation intensities, and grain properties undergo enormous transformation (as traced by infrared spectroscopy, (sub-)millimeter/centimeter interferometry and advanced disk modelling (Andrews and Williams, 2007; Bouwman et al., 2008; Andrews et al., 2009; Guilloteau et al., 2011; Williams and Cieza, 2011; Grady et al., 2013). The grain growth and sedimentation toward the midplane leads to more transparent and thus hotter disk atmosphere and flatter vertical structure, shrinking the zone when gas and dust are collisionally coupled and have similar temperatures. The disk chemical composition changes along with the evolution of the physical conditions (Aikawa and Nomura, 2006; Nomura et al., 2007; Cleeves et al., 2011; Ilee et al., 2011; Fogel et al., 2011; Vasyunin

et al., 2011; *Akimkin et al.*, 2013). As a result of the increasing X-ray/UV-irradiation with time, the molecularly-rich, warm layer shifts closer to the cold midplane and the pace of surface chemistry can be delayed by the grain growth.

6.2. Deuterium fractionation

Observational studies of the detailed chemical structure of protoplanetary disks require high sensitivity and high angular resolution measurements, which started to become available only in the past few years. For this reason, measurements of deuterium fractions are very sparse and so far limited to two PSN analogue disks (the T Tauri disks TW Hya and DM Tau) and one disk around a $2 M_{\odot}$ star (the Herbig Ae star HD 163296; *Mathews et al.* (2013), not discussed here).

TW Hya. The first deuterated molecule, DCO^+ , was detected by *van Dishoeck et al.* (2003) in the T Tauri star TW Hya. The $\text{DCO}^+/\text{HCO}^+$ abundance ratio was found $\simeq 0.04$, similar to that measured toward pre-stellar cores (§4). The first image of the DCO^+ emission has been obtained by *Qi et al.* (2008a) using the Submillimeter Array (SMA). They found variations of the $\text{DCO}^+/\text{HCO}^+$ across the disk, increasing outward from $\sim 1\%$ to $\sim 10\%$ and with a rapid falloff at radii $\gtrsim 90$ AU. DCN/HCN was also measured in the same observing run and found to be $\simeq 2\%$. Combining SMA with ALMA data, *Öberg et al.* (2012) have inferred that DCO^+ and DCN do not trace the same regions: DCN is centrally concentrated and traces inner zones. This is in agreement with the theoretical predictions that DCN can also be produced in gas warmer than 30 K via the intermediate molecular ion CH_2D^+ (see §2.1), unlike DCO^+ which is linked to H_2D^+ . The CO snow line has been recently imaged using ALMA observations of N_2H^+ (a molecular ion known to increase in abundance when CO starts to freeze-out, as CO is one of the destruction partners), finding a radius of ~ 30 AU (*Qi et al.*, 2013). Deuterated species are expected to thrive close to the CO snow line and more observations should be planned to improve our understanding of the deuterium fractionation around this disk.

DM Tau. *Guilloteau et al.* (2006) found a $\text{DCO}^+/\text{HCO}^+$ abundance ratio toward DM Tau ($\simeq 0.004$) about one order of magnitude lower than toward TW Hya, indicating interesting differences between apparently similar sources, which need to be explored in more detail.

6.3. Origin of the deuterium fractionation

The deuterium fractionation in protoplanetary disks is expected to occur mainly in the cold ($T \lesssim 30$ K) midplane region, where the CO freeze-out implies large abundances of the H_3^+ deuterated isotopologues (*Ceccarelli and Dominik*, 2005). The fractionation route based on CH_2D^+ is also effective in the warm inner disk midplane and molecular layer (Fig.7 and §2). Modern models of protoplanetary disks include a multitude of deuterium fractionation reactions and multiply-deuterated species, still however without nuclear spin-state processes.

Willacy (2007) have investigated deuterium chemistry in the outer disk regions. They found that the observed $\text{DCO}^+/\text{HCO}^+$ ratios can be reproduced, but, in general, the deuteration of gaseous molecules (in particular doubly deuteration) can be greatly changed by chemical processing in the disk. In their later study, *Willacy and Woods* (2009) have investigated deuterium chemistry in the inner 30 AU, using the same physical structure and accounting for gas and dust thermal balance. While a good agreement between the model predictions and observations of several non-deuterated gaseous species in a number of protoplanetary disks was obtained, the calculated D/H ratios for ices were higher than measured in the Solar System comets.

Thi et al. (2010b) have focused on understanding deuterium fractionation in the inner warm disk regions and investigated the water D/H ratio in dense ($\gtrsim 10^6 \text{ cm}^{-3}$) and warm ($\sim 100 - 1000$ K) gas, caused by photochemistry and neutral-neutral reactions. Using the T Tau disk structure calculated with “ProDiMo” (*Woitke et al.*, 2009), they predicted that in the terrestrial planet-forming region at $\lesssim 3$ AU the water D/H ratio may reach $\sim 1\%$, which is higher than the value of $\approx 1.5 \times 10^{-4}$ measured in the Earth ocean water (Tab. 1). As mentioned in §2.2, the formation of HDO at high temperatures ($\gtrsim 100$ K) proceeds through the $\text{OH} + \text{HD} \rightarrow \text{OD} + \text{H}_2$ reaction (see Fig.2).

As presented above, our knowledge on deuterium chemistry in protoplanetary disks, particularly from the observational perspective, is still rather poor. Only the deuterated molecules DCN and DCO^+ have been detected so far (plus the recent Herschel detection of HD toward TW Hya; *Bergin et al.*, 2013). The analysis of their relatively poorly resolved spectra shows that DCO^+ emission tends to peak toward outer colder disk regions, while DCN emission appears to be more centrally peaked. Their chemical differentiation seems to be qualitatively well-understood from the theoretical point of view, with DCN being produced at warmer temperatures ($\lesssim 70 - 80$ K) by fractionation via CH_2D^+ and C_2HD^+ , and DCO^+ being produced at cold temperatures ($\lesssim 10 - 30$ K) by fractionation via H_3^+ isotopologues. However, theoretical models of the inner warm disk regions still tend to overpredict the D/H ratios of molecules observed in comets. ALMA, soon in full capabilities, will provide us with a wealth of new precious data on deuterated species in many protoplanetary disks, which will shed light on the chemical and physical processes during this delicate phase of planet formation.

7. COMETS

7.1. The origin of comets

Having retained and preserved pristine material from the Proto Solar Nebula (PSN) at the moment of their accretion, comets contain unique clues to the history and evolution of the Solar System. Their study provides the natural link between interstellar matter and Solar System bodies and their formation. Comets accreted far from the Sun, where ices could condense, and have remained for most of their life-

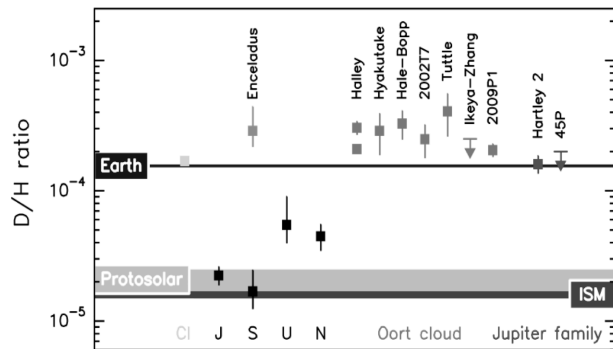


Fig. 8.— D/H ratio in the water of comets compared to values in carbonaceous meteorites (CI), Earth’s oceans (VSMOW; see Tab. 1), and Enceladus. Displayed data for planets, the interstellar medium, and the PSN refer to the value in H_2 (see text for details). Adapted from *Lis et al.* (2013).

time outside the orbit of Pluto. According to the reference scenario, the Oort cloud, which is the reservoir of long-period comets (also called OCC), was populated by objects gravitationally scattered from the Uranus-Neptune region, with some contribution from the Jupiter-Saturn region (*Dones et al.*, 2004; *Brasser*, 2008). The reservoir of ecliptic short-period comets (the so-called Jupiter-family comets JFC) is the Kuiper belt beyond Neptune, more precisely the scattered disk component of that population characterized by highly eccentric orbits (*Duncan and Levison*, 1997). In the current picture described by the Nice model, the present scattered disk is the remnant of a much larger scattered population produced by the interaction of the primordial planetesimal disk with a migrating Neptune. In the simulations of *Brasser and Morbidelli* (2013) made in the framework of the Nice model, the Oort cloud and the scattered disk formed simultaneously from objects from the same parent population. In summary, either the two comet reservoirs come from the same population of objects formed in the Uranus-Neptune zone, or Oort-cloud comets formed on average closer to the Sun. Finally, a third option reported in the literature is that Oort-cloud comets were captured from other stars when the Sun was in its birth cluster (*Levison et al.*, 2010). The molecular and isotopic composition in these two reservoirs can provide key answers in this respect.

7.2. Deuterium fractionation

Because of the faint signatures of deuterated species, data were only obtained in a handful of bright comets. The first measurements of the D/H ratio in cometary H_2O were obtained in comet 1P/Halley from mass-resolved ion-spectra of H_3O^+ acquired with the Ion Mass Spectrometer (*Balsiger et al.*, 1995) and the Neutral Mass Spectrometer (*Eberhardt et al.*, 1995) instruments onboard the European Giotto spacecraft. These independent data provided precise D/H values of $(3.08^{+0.38}_{-0.53}) \times 10^{-4}$ and $(3.06 \pm 0.34) \times 10^{-4}$ (*Balsiger et al.*, 1995; *Eberhardt et al.*, 1995). We

note however that *Brown et al.* (2012) reexamined the mass-spectrometer measurements, reevaluating these values to 2.1×10^{-4} .

From observations undertaken with CSO and JCMT, HDO was detected in the bright long-period comets C/1996 B2 (Hyakutake) and C/1995 O1 (Hale-Bopp) from its $1_{01}-0_{00}$ line at 464.925 GHz (*Bockelée-Morvan et al.*, 1998; *Meier et al.*, 1998a). The derived D/H values ($(2.9 \pm 1.0) \times 10^{-4}$ and $(3.3 \pm 0.8) \times 10^{-4}$, for comets Hyakutake and Hale-Bopp, respectively) are in agreement with the determinations in comet Halley (Fig. 8). Finally, observations of the HDO $1_{10}-1_{01}$ transition at 509.292 GHz in the Halley-type comet 153P/Ikeya-Zhang yielded $\text{D/H} < 2.5 \times 10^{-4}$ (*Biver et al.*, 2006).

Using the new high resolution spectrograph CRIRES of the ESO VLT, *Villanueva et al.* (2009) observed the HDO ro-vibrational transitions near $3.7 \mu\text{m}$ in the Halley-family comet 8P/Tuttle originating from the Oort cloud. Twenty three lines were co-added to get a marginal detection of HDO, from which a formal value of D/H of $(4.09 \pm 1.45) \times 10^{-4}$ was derived.

In cometary atmospheres, water photodissociates into mainly OH and H. The OD/OH ratio was measured to be $(2.5 \pm 0.7) \times 10^{-4}$ in the Oort-Cloud comet C/2002 T7 (LINEAR) through ground-based observations of the OH $A^2\Sigma^+ - X^2\Pi_i$ ultraviolet bands at 310 nm obtained with VLT feeding the UVES spectrograph (*Hutsemékers et al.*, 2008). No individual OD line was detected, but a marginal 3σ detection of OD was obtained by co-adding the brightest lines. Atomic deuterium (D) emission was also discovered during ultraviolet observations of comet C/2001 Q4 (NEAT) in April 2004 using the spectrograph STIS of the Hubble Space Telescope (*Weaver et al.*, 2008). The Lyman- α emission from both D and atomic hydrogen were detected, from which a preliminary value $\text{D/H} = (4.6 \pm 1.4) \times 10^{-4}$ was derived, assuming that H_2O is the dominant source of the observed D and H, as is likely the case. The strength of the optical method is that both normal and rare isotopologues have lines in the same spectral interval and are observed simultaneously, avoiding problems related to comet variable activity.

The most recent D/H measurements in cometary water were acquired using the ESA Herschel satellite. The HDO $1_{10}-1_{01}$ transition at 509.292 GHz was observed using the HIFI spectrometer in the Jupiter-family comets 103P/Hartley 2 and 45P/Honda-Mrkos-Pajdušáková (*Hartogh et al.*, 2011; *Lis et al.*, 2013), and in the Oort-cloud comet C/2009 P1 (Garradd) (*Bockelée-Morvan et al.*, 2012). Observations of HDO were interleaved with observations of the H_2O and H_2^{18}O $1_{10}-1_{01}$ lines. Since the H_2O ground state rotational lines in comets are optically thick, optically thin lines of H_2^{18}O provide, in principle, a more reliable reference for the D/H determination. The $\text{HDO}/\text{H}_2^{18}\text{O}$ was measured to be 0.161 ± 0.017 for comet Hartley 2, i.e., consistent with the VSMOW (0.1554 ± 0.0001). The $\text{HDO}/\text{H}_2^{18}\text{O}$ value of 0.215 ± 0.023 for comet Garradd suggests a significant difference ($3-\sigma$) in deuterium

Comet	D/H	Type
Halley	$(3.1 \pm 0.5) \times 10^{-4}$	OCC
Hyakutake	$(2.9 \pm 1.0) \times 10^{-4}$	OCC
Hale-Bopp	$(3.3 \pm 0.8) \times 10^{-4}$	OCC
2002 T7	$(2.5 \pm 0.7) \times 10^{-4}$	OCC
Tuttle	$(4.1 \pm 1.5) \times 10^{-4}$	OCC
Ikeya-Zhang	$\leq 2.5 \times 10^{-4}$	OCC
2009 P1	$(2.06 \pm 0.22) \times 10^{-4}$	OCC
2001 Q4	$(4.6 \pm 1.4) \times 10^{-4}$	OCC
Hartley 2	$(1.61 \pm 0.24) \times 10^{-4}$	JFC
45P	$\leq 2.0 \times 10^{-4}$	JFC

Table 3: Summary of the measured water D/H values in comets (see text for the references). The last column report the type of comet, Oort-cloud (OCC) or Jupiter-family (JFC).

content between the two comets. *Hartogh et al.* (2011) derived a D/H ratio of $(1.61 \pm 0.24) \times 10^{-4}$ for comet Hartley, assuming an $\text{H}_2^{16}\text{O}/\text{H}_2^{18}\text{O}$ ratio of 500 ± 50 , which encompasses the VSMOW value and values measured in cometary water (*Jehin et al.*, 2009). For comet Garradd, the derived D/H ratio is $(2.06 \pm 0.22) \times 10^{-4}$ based on the $\text{HDO}/\text{H}_2^{16}\text{O}$ production rate ratio, and $(2.15 \pm 0.32) \times 10^{-4}$, using the same method as *Hartogh et al.* (2011). Herschel observations in the Jupiter family comet 45P/Honda-Mrkos-Pajdušáková were unsuccessful in detecting the HDO 509 GHz line, but resulted in a sensitive 3σ upper limit for the D/H ratio of 2.0×10^{-4} which is consistent with the value measured in comet 103P/Hartley 2 and excludes the canonical pre-Herschel value measured in Oort-cloud comets of $\sim 3 \times 10^{-4}$ at the 4.5σ level (*Lis et al.*, 2013).

Besides H_2O , the D/H ratio was also measured in HCN, from the detection of the J=5–4 rotational transition of DCN in comet Hale-Bopp with the JCMT (*Meier et al.*, 1998b). The inferred D/H value in HCN is 2.3×10^{-3} , i.e., seven times the value measured in water in the same comet. Finally, D/H upper limits for several molecules were obtained, but most of these upper limits exceed a few percent (*Crovisier et al.*, 2004). For CH_4 , observed in the near-IR region, the most stringent D/H upper limits are $\sim 0.5\%$ (*Gibb et al.*, 2012, and references therein).

Table 3 summarizes the situation and Fig. 8 shows the water ice D/H values measured so far in comets, compared to the protosolar and the Earth ocean’s value VSMOW (see Tab. 1). Isotopic diversity is present in the population of Oort-cloud comets, with members having a deuterium enrichment of up to a factor of two with respect to the Earth value. The only two Jupiter-family comets for which the D/H ratio has been measured present low values consistent with the Earth’s ocean value.

7.3. Origin of the deuterium fractionation

The high D/H ratio measured in comets cannot be explained by deuterium exchanges between H_2 and H_2O in the PSN, and is interpreted as resulting from the mixing of

D-rich water vapor originating from the pre-solar cloud or outer cold disk, and material reprocessed in the inner hot PSN (§9). The discovery of an Earth-like D/H ratio in the Jupiter-family comet 103P/Hartley 2 came as a great surprise. Indeed, Jupiter-family comets were expected to have D/H ratios higher than or similar to Oort-cloud comets according to current scenarios (*Kavelaars et al.*, 2011), implying that the source regions of these two populations or the models investigating the gradient of D/H in the PSN should be revisited. Actually, the only dynamical theory that could explain in principle an isotopic dichotomy in D/H between Oort-cloud and Jupiter-family comets is the one arguing that a substantial fraction of Oort-cloud comets were captured from other stars when the Sun was in its birth cluster (*Levison et al.*, 2010). Another possible solution is that there was a large-scale movement of planetesimals between the inner and outer PSN. According to the Grand Tack scenario proposed for the early Solar System, when the giant planets were still embedded in the nebular gas disk, there was a general radial mixing of the distribution of comets and asteroids (*Walsh et al.*, 2011). Both the similarity of the D/H ratio in comets 103P/Hartley 2 and 45P/Honda-Mrkos-Pajdušáková with that found in carbonaceous chondrites, and the isotopic diversity observed in the Oort-cloud population would be in agreement with this scenario, though D/H variations in the Jupiter family might be expected as well. Finally, another possibility is a non monotonic D/H ratio as a function of the heliocentric distance, as predicted by models considering a residual infalling envelope surrounding the PSN disk (*Yang et al.*, 2013). Section 9 will explore in greater detail these models.

8. CARBONACEOUS CHONDRITES AND INTER-STELLAR DUST PARTICLES

Meteorites have fallen to the Earth throughout its history. Interplanetary Dust Particles (IDPs) are collected in the stratosphere or in the ices of the Earth polar regions. While most IDPs are believed to be cometary fragments, probably from Jupiter-Family comets (*Nesvorný et al.*, 2010), meteorites are fragments of main-belt asteroids (2–4 AU; *Morbidelli et al.*, 2000), with the few exceptions of martian and lunar meteorites. Both meteorites and IDPs provide us with a huge amount of information on the early phases of the Solar System formation. Among the various groups of meteorites (see for example the review by *Alexander*, 2011), the carbonaceous chondrites (CCs) are believed to be the more pristine, little altered by parent bodies, so that we will focus this section on this group. Briefly, CCs are stony fragments of primitive asteroids of near solar bulk composition that were not much heated or differentiated. It is in these mineral matrixes that clay minerals (the so-called phyllosilicates) and diverse soluble and insoluble organic materials are found. Based on the techniques used to study it, the organic matter is classified as Insoluble Organic Matter (IOM) and Soluble Organic Compounds (SOC; sometime this is also referred as Soluble Organic Matter or SOM). The pos-

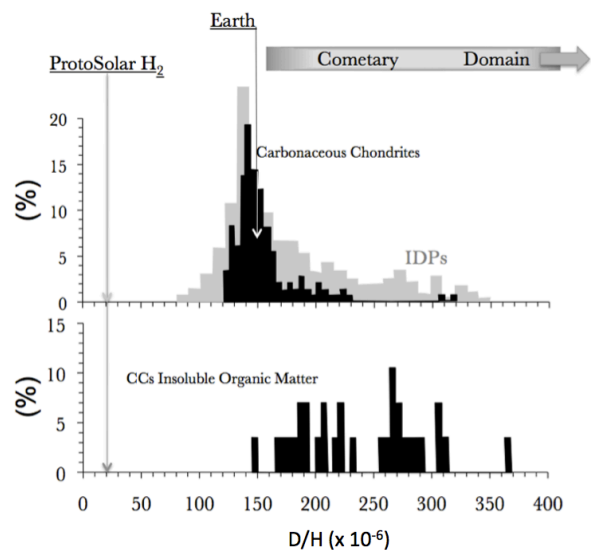


Fig. 9.— Histograms of the D/H ratio in CCs (upper panel, black), in IDPs (upper panel, grey) and in the IOM lower panel). The figure also shows the PSN and terrestrial water D/H ratios (Tab. 1). Note that the D/H ratios measured in the IOM “hot spots” are not reported here. The figure is based on the personal compilation of F. Robert and includes published measurements up to June 2013.

sible interdependence between minerals and organic materials through their Solar and pre-Solar formative history is not known and remains one unexplained feature of chemical evolution. Evidence of CCs exposure to liquid water also indicates that aqueous processes and partaking minerals contributed to their final organic inventory. In this section, we describe the deuterium fractionation in the clays, IOM, and SOC separately.

8.1. Clays minerals in Carbonaceous Chondrites and Interplanetary Dust Particles

For more than two decades (Robert *et al.*, 1979), it has been known that CC clay minerals exhibit a systematic enrichment in deuterium relative to the PSN D/H ratio (Tab. 1). Similarly, clays in IDPs are enriched in deuterium (Zinner *et al.*, 1983; Messenger, 2000; Aléon *et al.*, 2000). Figure 9 shows the distribution of the bulk D/H ratio in the CCs and IDPs. In CCs, the contribution of the D-rich organic matter (see below) to the variations of the bulk D/H ratio is negligible relative to the large domain of isotopic variations, i.e. $\leq 1.5 \times 10^{-5}$. However, for IDPs, the relative contribution of organic H to hydroxyls is not well known so that the tail in the D/H distribution towards the high values may be caused by the contribution of D-rich organic hydrogen. Both CCs and IDPs have D/H ratios ~ 7 times larger than the PSN. Their D/H distribution is peaked around the value of the terrestrial oceans, the VSMOW (Tab. 1), with a shoulder extending up to about 3.5×10^{-4} . The majority of CCs and IDPs possesses, therefore, a D/H ratio lower than that measured in most comets (§7).

Alexander *et al.* (2012) recently discovered a correlation between the D/H ratio and the amount of organic hydrogen relative to the bulk hydrogen (which, as mentioned above, is dominated by the hydroxyl groups of clays), indicating that the water *in the meteorite parent body* had a D/H ratio - prior to isotopic exchange with deuterium-rich organics - as low as 9.5×10^{-5} , namely smaller than the SWOM value. In addition, these authors found that the D/H ratio of this pristine water varies according to the meteorite class, indicating different degree of isotopic enrichment of the PSN water prior to its introduction in the CCs parent bodies. Based on these findings, these authors propose that the original D/H ratio in meteoritic water (i.e. before the clay formation) is, therefore, smaller than what is measured nowadays, with consequences on the terrestrial water origin (§10.3).

8.2. Insoluble Organic Matter

IOM represents the most abundant (70–90%) form of carbon isolated from CCs (Bitz and Nagy, 1966). It is mostly composed by carbon rings and chains, as shown in Fig. 10, and contains several other atoms: O, N, S, and P (Remusat *et al.*, 2005; Cody and Alexander, 2005; Robert and Derenne, 2006; Derenne and Robert, 2010). Note, however, that the molecular structure sketched in the figure should not be regarded as an organic formula of the IOM, but rather as a statistical representation of the relative abundances of the organic bonds in the IOM. In addition, a study by Cody *et al.* (2011) showed a molecular relationship between chondritic and cometary organic solids. Remarkably, the possible molecular structure of interstellar refractory organic, namely Poly Aromatic Hydrocarbons (PAHs), seems to be quite different from that of the IOM (Kwok, 2004; Remusat *et al.*, 2005). What is the origin of this difference is still an open issue: it may hint to a different origin of the two or to a substantial restructuring of PAHs on the protosolar grains.

Studies of the molecular deuteration in the IOM have been carried out by several groups and with a variety of techniques used in organic chemistry (Robert and Epstein, 1982; Yang and Epstein, 1983; Alexander, 2011). Also in this case, high values have been measured, as summarised in Fig. 9. However, contrarily to the CCs clay minerals and IDPs, the D/H distribution is not peaked around the terrestrial value but rather spread from 1.5 to $\sim 3.7 \times 10^{-4}$. Besides, the measured values are larger than those in CCs bulk (dominated by clay minerals, see above), IDPs and Earth and more similar to what measured in cometary water (Fig. 9). As discussed in §5, the difference between water and organic deuterium fractionation in protostellar sources, where water is systematically less deuterated, has been interpreted as due to a different history of the water and the organic species formation on the grain surfaces. This may also be the case for the water and organic material in CCs and IDPs as we will discuss in the following.

Remarkably, Remusat *et al.* (2006, 2009, 2012) have dis-

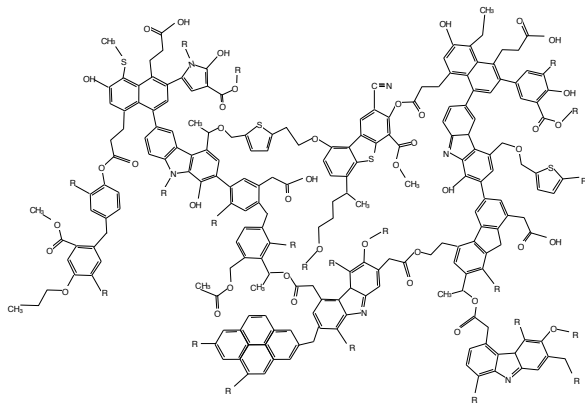


Fig. 10.— Statistical model of the molecular structure of the IOM isolated from the Murchison CC. The “R” marks the presence of an unknown organic groups, called moiety. Adapted from *Derenne and Robert (2010)*.

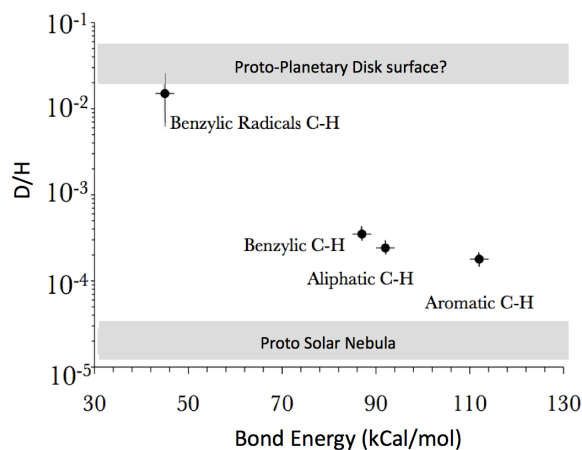


Fig. 11.— Measured D/H ratio in functional groups as function of the bond energy of the group.

covered a relation between the D/H ratio measured in the IOM and the energy of the different C-H bonds, namely aromatic (protonated carbon in aromatic moieties), aliphatic (in chains linking aromatic moieties) and benzylic bonds (in the alpha position of the cycles). In addition to these three bonds, the D/H ratio of the benzylic carbons attached to aromatic radicals has been measured through Electron Paramagnetic Resonance (EPR). These radicals are considerably enriched in deuterium, with $D/H = (1.5 \pm 0.5) \times 10^{-2}$ (cf. Fig. 5; *Gourier et al., 2008*). This is the largest deuterium enrichment measured in the primitive objects of the Solar System. The occurrence of the so-called “deuterium hot-spots” observed with the NanoSims technique and that are dispersed in the IOM, is ascribed to a local micrometer size concentration of these radicals among the molecular network of the IOM (*Remusat et al., 2009*).

The relation between the measured D/H and the energy of the bond is shown in Fig. 11: the larger the bond energy, the smaller the measured D/H. This relation between the

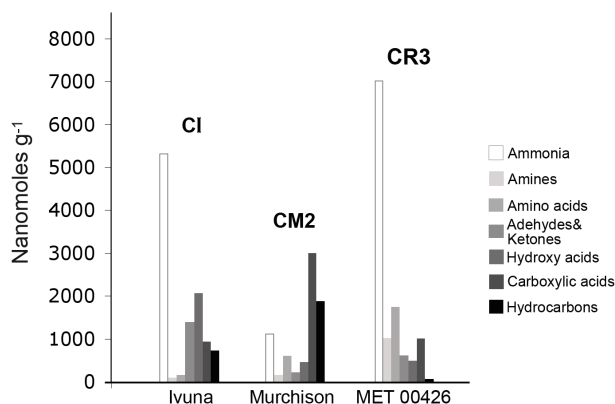


Fig. 12.— Abundance distribution of soluble organic compounds in different types of CCs (Carbonaceous Chondrites) meteorites (CI: Ivuna-type; CM: Mighei-type; CR: Renazzo-type; MET: Meteorite Hills). In general, numbers 1-3 indicate asteroidal aqueous alteration extent, where 3 means least altered.

energy bond and the deuterium fractionation led *Remusat et al. (2006)*; *Gourier et al. (2008)*; *Derenne and Robert (2010)* to propose that the deuteration of the IOM occurred during the protoplanetary disk phase of the Solar System rather than during the pre-/proto- stellar phase or during the parent body metamorphism (see §9).

8.3. Soluble Organic Compounds

The distribution of the most abundant species of CC soluble compounds is shown in Fig. 12. Besides the ones shown, more molecules of diverse composition were identified, such as di- and poly- carboxylic acids, polyols, imides and amides (*Pizzarello et al., 2006*, and references therein), nucleobases (*Callahan et al., 2011*), and innumerable others are implied by spectroscopy (*Schmitt-Kopplin et al., 2010*). Their distributions vary significantly between CCs, e.g., ammonia and amino acids are the most abundant compounds in Renazzo-type (CR) but hydrocarbons are in Mighei-type (CM) meteorites.

Amid this complex suite, amino acids (*aa*) appear to carry a unique prebiotic significance because of their essential role as constituent of proteins in the extant biosphere. Moreover, meteoritic amino acids may display chiral asymmetry in similarity with their terrestrial counterparts (*Pizzarello and Groy, 2011*, and references therein), suggesting that abiotic cosmochemical processes might have provided the early Earth with a primed inventory of exogenous molecules carrying an evolutionary advantage. The amino acids of CCs comprise a numerous and diverse group, having linear or branched alkyl chains and primary as well as secondary amino groups (Fig. 13) in different positions along those chains. These subgroups may require different pathways of formation and/or precursor molecules; all are enriched in ^{13}C , ^{15}N and D and appear to have their own isotopic signatures. This isotopic diversity was first made

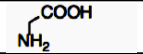
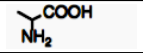
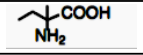
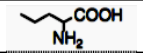
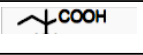
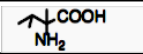
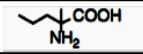
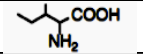
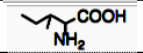
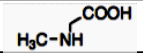
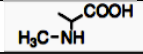
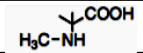
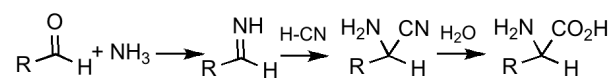
AMINO ACID		CM2 (δD or D/H in 10^{-4})	CR2 (δD or D/H in 10^{-4})
Linear alkyl chain compounds			
glycine		366-399 or 2.12-2.17	868-1070 or 2.89-3.21
DL alanine		360-765 or 2.11-2.74	1159-1693 or 3.35-4.17
DL-2-a. butyric		1091-1634 or 3.24-4.08	1920-3409 or 4.53-6.63
norvaline		1505 or 3.88	nd
Branched chain compounds			
2-a. isobutyric		2362-3097 or 5.21-6.35	4303-7257 or 8.22-12.80
isovaline		2081-3419 or 4.78-6.85	3813-7050 or 7.46-12.48
DL-valine		1216-2432 or 3.43-5.32	2086-3307 or 4.78-6.68
2-a. 2,3 methylbutyric		3318-3604 or 6.69-7.14	nd
DL-2methylnorvaline		2686-3021 or 5.71-6.23	nd
DL-allo isoleucine		2206-2496 or 4.97-5.42	nd
L-leucine		1792-1846 or 4.33-4.41	nd
N-substituted amino acids			
Sarcosine		1274-1400 or 3.52-3.72	nd
DL-N-methylalanine		1224-1310 or 3.44-3.58	nd
N-methyl-2am. isobutyric		3431-3461 or 6.87-6.91	nd

Fig. 13.— Range of δD ‰ values (see Tab. 1 for definition) and in D/H units of 10^{-4} determined for meteoritic 2-amino, and 2-methylamino acids, by compound-specific isotopic analyses for CM2 (Murchison, Murray and Lonewolf Nunataks 94101) and CR2 (for Graves Nunataks 95229 and Elephant Morains 92042). Data are from Pizzarello and Huang (2005) and Elsila *et al.* (2012). nd= not determined.

evident by the varying $\delta^{13}\text{C}$ values detected for Murchison *aa* (+4.9 to +52.8) and the significant differences found within and between *aa* subgroups; e.g., the ^{13}C content of 2-amino acids (Fig. 13) declines with chain length, as seen for carboxylic acids and alkanes, while 2-, 3-, and 4-amino-, or dicarboxylic amino acids do not have similar trends. Also 2-methyl-2-amino acids are more enriched in ^{13}C than the corresponding 2-H homologues (Pizzarello *et al.*, 2004). The δD values, determined for a larger number of *aa* in several meteorites (Fig. 13), show that *aa* subgroups are isotopically distinct in regard to this element as well and reveal additional differences amongst types of meteorites: again, branched *aa* display the largest δD values. A higher D-content of branched alkyl chains was seen also in all other *aa* sub-groups analyzed, i.e., in the dicarboxylic *aa* and 3-, 4-, 5-amino compounds.

The locales, precursor molecules and synthetic processes

that might account for meteoritic *aa* molecular, isotopic and chiral properties are still being debated and have been only in part elucidated. As for their synthetic pathways, the first analytical indication came from the finding in meteorites of similar suites of hydroxy-, and amino acids, which led Peltzer and Bada (1978) to propose a Strecker-type synthesis for both compound groups:



The reaction proceeds via the addition of HCN to aldehydes and ketones in the presence of ammonia and water; the larger the ammonia abundance, the larger the expected ratio of NH_2 -/ OH -acids, the latter being the only compounds formed in ammonia absence. The scheme agrees with many data from CCs analyses but was further corrob-

orated recently by enantiomeric excesses observed in the 6C *aa* isoleucine of several meteorites (Pizzarello *et al.*, 2012), which demonstrated the possible origin and survival of enantiomeric excesses from their precursor aldehyde.

A Strecker synthesis readily accounts for meteoritic *aa* large D/H ratios: all reactants necessary for its first phase have been detected in interstellar clouds and are highly deuterated. The incorporation of little-altered interstellar species into volatile-rich CC parent bodies would then provide the subsequent aqueous phase.

The possible reliance upon minerals by organic materials through their Solar and pre-Solar formative history is not known and remains one unexplained feature of chemical evolution. For carbonaceous meteorites, evidence of CC exposure to liquid water indicates that aqueous processes and partaking minerals contributed to their final organic inventory.

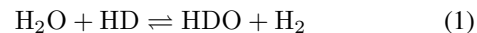
9. THE PROTO SOLAR NEBULA MODELS

In this section we discuss separately the models that have been proposed to explain the measured deuterium fractionation of water and organics in comets, CCs and IDPs. As in the relevant literature, we will use the enrichment factor f , defined as the ratio between the water D/H and the H₂ D/H of the Proto Solar Nebula (PSN) (Tab. 1), which for the terrestrial evaporated water (VSMOW) is 7.

9.1. Deuterium fractionation of water

The PSN, namely the protoplanetary disk out of which the Earth formed, was initially composed of dust and gas (§6) with a D/H ratio close to the cosmic one ($\sim 2.1 \times 10^{-5}$ versus $\sim 1.6 \times 10^{-5}$; Tab. 1). As described in §2 to 6, several reactions in the pre-stellar to protoplanetary disk phases lead to the fractionation of deuterium of H-bearing species, and, in particular, of the water ice (§2.2). The planetesimals that eventually formed comets, the parent bodies of IDPs and meteorites, and possibly Earth (see the discussion in §10.3) were, therefore, covered by icy mantles enriched in deuterium. In the warm ($\gtrsim 100$ – 120 K) regions of the PSN, inside the snow-line, these ices sublimated. In general, PSN models aiming to model the fate of the ice (Drouart *et al.*, 1999; Mousis *et al.*, 2000; Mousis, 2004; Hersant *et al.*, 2001; Horner *et al.*, 2007, 2008; Kavelaars *et al.*, 2011) assumes that the PSN is a “diffusional” disk, in the sense that the turbulence is entirely responsible for its angular momentum transport. The first models used the simplest description for the disk provided by the famous α -viscosity 1D (vertical averaged) disk (Shakura & Sunyaev 1973). Later versions took into account the 2D structure of the disk (Hersant *et al.*, 2001). The viscosity, in the numerical models set by the value of α , is not only responsible for the mass accretion from the disk to the star (and, consequently, the disk thermal structure), but also for the dispersion of (part of) the angular momentum by diffusing matter outwards. From a chemical point of view, these models consider only the exchange of D-atoms between wa-

ter and molecular hydrogen through the reaction (Geiss and Reeves, 1981):



and consider the isotopic exchange proportional to the reaction rate, measured by *Lécluse and Robert* (1994), and the isotopic fractionation at equilibrium, measured by *Richet et al.* (1977). Therefore, in these models, the deuterium fractionation of water across the PSN depends on the deuterium exchange in the gas (where $T \gtrsim 200$ K) and the mixing of the outwards diffused D-unenriched water with the inwards diffused D-enriched water. At high temperatures ($\gtrsim 500$ K) this exchange leads to $f=1$, namely no water deuterium enrichment. At lower temperatures, the exchange leads to $f \leq 3$, but, being a neutral-neutral reaction, at temperatures $\lesssim 200$ K the reaction is too slow to play any role (Drouart *et al.*, 1999). Therefore, the deuterium fractionation of water across the PSN, in these models, depends on the deuterium exchange in the gas (where $200 \lesssim T \lesssim 500$ K) and the mixing of the outwards diffused D-enriched water (sublimated from the ices) with the D-unenriched gas. When the gas reaches a temperature equal to that of water condensation (which is a function of the heliocentric distance and time), the evolution of f in that point stops. It is then assumed that the ice D-enrichment is f and that any object formed at that distance will inherit the same enrichment. This implies that transport mechanisms of grains, such as turbulent diffusion or gas drag, are neglected and that there is no evolution afterwards (e.g., in cometary nuclei during their orbital evolution; *Brown et al.*, 2012). Figure 14 shows a cartoon of the situation.

In summary, these models, based on a strong assumption about the structure and dynamics of the PSN, depend on two basic parameters: the α value (or the turbulent viscosity prescription), which governs the thermal evolution of the disk and the diffusion, and the initial f profile before the disk evolution starts. Figure 15 shows the evolution of f as a function of the heliocentric distance as computed by *Kavelaars et al.* (2011). In this model, the initial f is constant across the disk and equal to the value found in LL3 meteorites (D/H=0.9– 7.3×10^{-4} ; *Deloué et al.*, 1998). The deuterium enrichment profile matches quite well the HDO/H₂O values measured in the Oort-cloud comets (§7), if they are formed in the Uranus/Neptune region as predicted by the Nice model (*Levison et al.*, 2008; *Brasser and Morbidelli*, 2013). The computed deuterium enrichment profile also matches the D/H value measured by the Cassini spacecraft in the plumes of Saturn’s satellite Enceladus at 10 AU, implying that the building blocks of this satellite may have formed at the same location as the Oort-cloud comets in the outer PSN (*Waite et al.*, 2009; *Kavelaars et al.*, 2011). However, the same model cannot reproduce the more recent HDO/H₂O value observed towards the Jupiter-Family comet 103P/Hartley (§7).

To solve this problem, *Yang et al.* (2013) developed a new model whose major differences with the models mentioned above are: (i) the PSN disk is not an isolated sys-

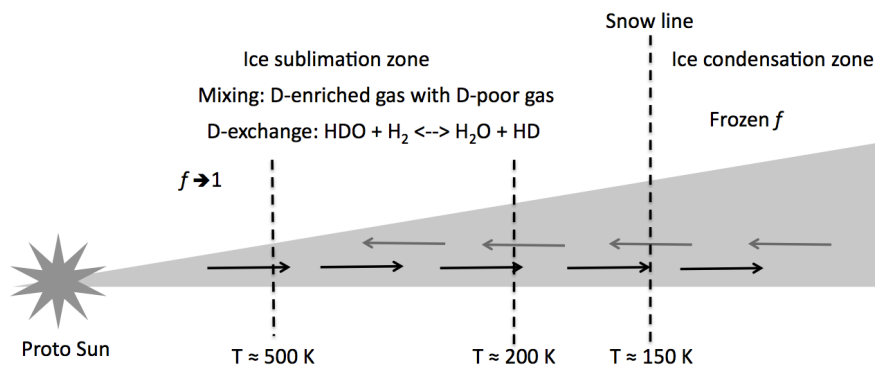


Fig. 14.— Cartoon of PSN models. The PSN is described as a turbulent disk where matter diffuses inwards and outwards. Inside the snow line, which moves outwards with increasing time, ices sublimate injecting D-enriched water vapour in the gas. The water vapour then exchanges the D-atoms with H_2 via the reaction $\text{H}_2\text{O} + \text{HD} \rightleftharpoons \text{HDO} + \text{H}_2$ where $T \gtrsim 200$ K. At $T \gtrsim 500$ K the exchange is very efficient and f tends to unity. When the outgoing gas reaches the condensation zone, it freezes out onto the grain ices. The acquired D-enrichment (f) is then conserved and inherited by the objects formed at that point.

tem but it is fed by the infalling surrounding envelope; (ii) the chemistry is not only governed by the H_2O – H_2 isotopic exchange, and other important reactions are taken into account, following the work by *Thi et al.* (2010b) (see also §6). The inclusion of fresh material from the envelope outer regions leads to a non-monotonic f profile (Fig. 16), contrarily to what predicted by the previous studies. This result stands also if the “old” chemical network, namely the isotopic exchange between water and hydrogen, is adopted. This non-monotonic gradient in deuteration could then explain the $\text{HDO}/\text{H}_2\text{O}$ ratio measured towards 103P/Hartley 2 and 45P/Honda-Mrkos-Pajdušáková.

Another important issue, raised by the asymmetric distribution of the water D/H in CCs and IDPs clays, has been recently addressed by *Jacquet and Robert* (2013). In this model, the initial D/H value in the water ice is assumed to be 3×10^{-4} , the average observed value in Oort cloud comets (§7). As in the previous models, iced grains drift inwards and vaporize at the snow line. Inside the snow line, the water vapor exchanges its D with H_2 and, as a result, the D/H ratio in water vapor decreases. Reaction kinetics compel isotopic exchange between water and hydrogen gas to stop at $T \sim 500$ K, well inside the snow line (~ 200 K). As a consequence, an isotopic gradient is established in the vapor phase between 200 K and 500 K by the mixing between the cometary source and the D/H ratio established at 500 K. The maximum value reached by the D/H ratio around the snow line is 1.2×10^{-4} . A fraction of this water having a D/H ratio of 1.2×10^{-4} can be transported beyond the snow line via turbulent diffusion where it (re)condenses as ice grains that are then mixed with isotopically comet-like water ($\text{D}/\text{H} \sim 3 \times 10^{-4}$). Thus, the competition between outward diffusion and net inward advection establishes an isotopic gradient, which is at the origin of the large isotopic variations in the carbonaceous chondrites and their

asymmetric distribution. Under this scenario, the calculated probability distribution function of the D/H ratio of ice mimics the observed distribution reported for CCs in Fig. 9. In this interpretation, the minimum D/H ratio of the distribution ($\sim 1.2 \times 10^{-4}$) corresponds to the composition of water (re)condensed at the snow line. The distribution function depends on several parameters of the model that are discussed by *Jacquet and Robert* (2013).

Interestingly, the presence of water on Earth, which exhibits a bulk (i.e., including surface water and mantle hydroxyls) D/H value of $1.49 \pm 0.03 \times 10^{-4}$ (*Lécuyer et al.*, 1998), can simply be accounted for by formation models advocating that terrestrial planets accreted from embryos sharing a CC composition (*Morbidelli et al.*, 2000). In this case, the contribution of comets to the Earth’s water budget would be relatively negligible.

9.2. Deuterium fractionation of organics

As discussed in §8, organic matter shows a systematic larger deuterium fractionation with respect to water (Fig. 9). A precious hint of what could be the reason for that is given by the relation between the energy of the functional group bond and the measured D/H value (Fig. 11). To explain this behaviour, several authors (*Remusat et al.*, 2006; *Gourier et al.*, 2008; *Derenne and Robert*, 2010) suggested that D-atoms are transmitted from HD to the organics via the H_2D^+ ions present in the disk (*Ceccarelli and Dominik*, 2005; *Qi et al.*, 2008b; *Willacy and Woods*, 2009, see also §6), basically following the scheme of Fig. 1. Laboratory experiments add support to this hypothesis. *Robert et al.* (2011) experimentally measured the exchange rate of D-atoms from H_2D^+ to organic molecules containing benzylic, aliphatic and aromatic bonds, finding relative ratios as measured in the IOM. Extrapolating to the typical conditions of protoplanetary disks, namely scaling to the the-

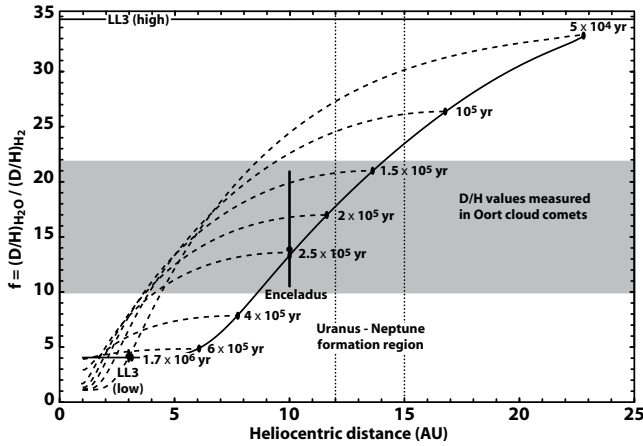


Fig. 15.— Enrichment factor f (Tab. 1) as a function of the heliocentric distance, as predicted by the *Kavelaars et al.* (2011) model. f increases in the gas (dashed curves) during the PSN diffusive phase evolution (Fig. 14; see text). The f increase stops when gas condenses (solid curve), which occurs at different times (marked as dots) for different heliocentric distances. The two horizontal lines marked with LL3 represent the D/H enrichments in LL3 meteorites, low and highly enriched components respectively. The vertical line marked Enceladus gives the range of f measured in this moon. The vertical dotted lines mark the region between Uranus and Neptune, where presumably the Oort cloud comets formed. The grey area corresponds to the f values measured in the Oort-cloud comets (Sec. 7).

oretical ion molecular ratio (i.e. to the $\text{H}_2\text{D}^+/\text{H}_2$ ratio) at the surface of the disk, these authors estimated that the exchange is very fast ($10^{4\pm 1}\text{yr}$) and, therefore, a plausible mechanism to occur. Therefore, the fact that the D/H distribution for the IOM is systematically enriched in D compared with that for water (cf. Fig. 9) could result from reactions in the gas phase and not connected with a fluid circulating in parent body meteorites during a hydrothermal episode. Indeed, all known isotopic reactions of organic molecules with a fluid should have resulted in the opposite distribution i.e., a systematic depletion in the organic D/H ratio compared with that of clays.

10. FOLLOWING THE UNROLLED DEUTERIUM THREAD

10.1. Overview of the deuterium fractionation through the different phases

Figure 17 graphically summarises the measured values of the D/H ratio from pre-stellar cores up to Solar System bodies, whereas Table 4 lists the measured D/H values and the main characteristics of the observations of Solar System bodies. Overall, the figure and the table, together with Fig. 9, raise a number of questions, often found in the literature too, which we address here.

1. Why is the D/H ratio systematically lower in Solar Sys-

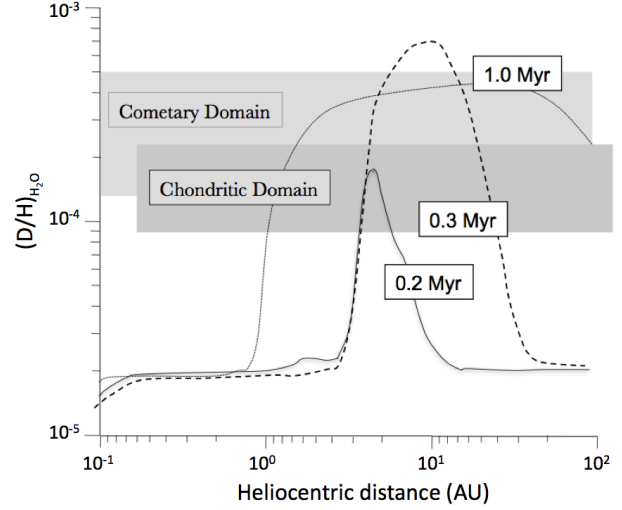


Fig. 16.— The radial distribution of D/H in the PSN at different epochs of its evolution (adapted from *Yang et al.*, 2013). Jupiter-family comets, presumably formed in the trans-Neptunian region, are predicted to have a lower D/H ratio than the Oort cloud comets, presumably in majority formed in the Uranus/Neptune region.

tem bodies than in pre- and proto- stellar objects? When and how did this change occur?

May be here the answer is, after all, simple. All the Solar System bodies examined in this chapter (meteorites and comets) were originally at distances less than 20 AU from the Sun. The D/H measurements of all pre- and protostellar objects examined in this chapter (pre-stellar cores, protostars and protoplanetary disks) refer to distances larger than that, where the temperatures are lower and, consequently, the deuteration is expected to be much larger (§2.1). Therefore, this systematic difference may tell us that the PSN did not undergo a global scale re-mixing of the material from the outer ($\gtrsim 20$ AU) to the inner regions. There are exceptions, though, represented by the “hot spots” in meteorites, which, on the contrary, may be the only representatives of this large scale re-mixing of the material in the PSN.

2. Why does organic material have a systematically higher D/H value than water, regardless the object and evolutionary phase?

The study of the deuterium fractionation in the pre-stellar cores (§4) and protostars (§5) has taught us that the formation of water and organics in different epochs is likely the reason why they have a different D/H ratio (Fig. 5). Water ices form first, when the density is relatively low ($\sim 10^4 \text{cm}^{-3}$) and CO not depleted yet, so that the $\text{H}_2\text{D}^+/\text{H}_3^+$ ratio is moderate (§2.1). Organics form at a later stage, when the cloud is denser ($\gtrsim 10^5 \text{cm}^{-3}$) and CO (and other neutrals) condenses on the grain surfaces, making possible a large enhancement of the $\text{H}_2\text{D}^+/\text{H}_3^+$. Can this also explain, *mutatis mutandis*, the different deuterium fractionation of water and organics measured in CCs and comets? After all,

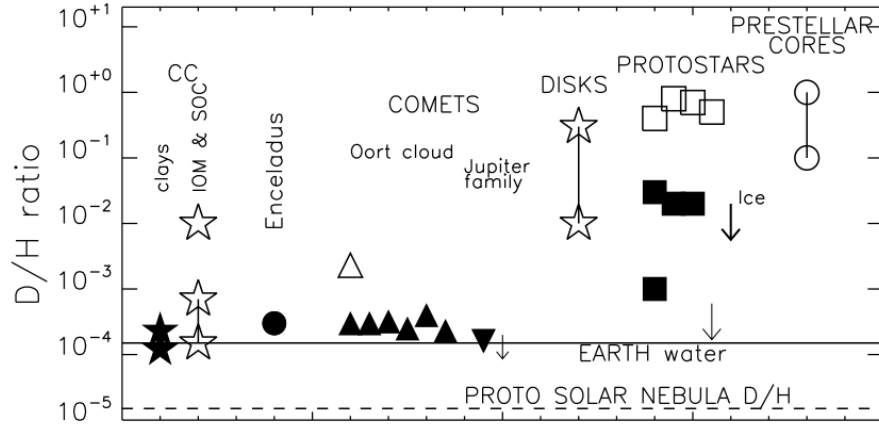


Fig. 17.— D/H ratio in the Solar System objects and astronomical sources. The filled symbols refer to water measures whereas open symbols refer to organic matter. The different objects are marked.

Object	D/H [$\times 10^{-4}$]	Note
Oort-Cloud Comets ^a	~ 3	Measured in seven comets.
Jupiter-Family Comets ^a	≤ 2	Measured in two comets: 1.61 ± 0.24 and ≤ 2 .
IDPs ^a	1.5–3.5	The D/H distribution is peaked at 1.3, with a shoulder from 0.8 to 3.5 (it mimics the CC clays D/H distribution).
CC clays ^a	1.2–2.3	The D/H distribution is peaked at 1.4, with a shoulder from 1.7 to 2.3.
CC IOM ^b	1.5–3.5	The D/H distribution does not have a peak.
CC IOM functional groups ^b	1.5–5.5	The larger the functional group bonding energy the larger the D/H.
CC IOM deuterium hot spots ^b	~ 100	Micrometer size spots in the IOM networks where D/H is highly enhanced.
CC SOC ^b	2.1–7.1	Branched <i>aa</i> show the largest D/H.

Table 4: Main characteristics of deuteration fractionation in comets and carbonaceous chondrites (CC). For explanations and references, see Secs. 7–8. Notes: ^aHDO/H₂O; ^bdeuterium fractionation in organics;

if the PSN cooled down from a hot phase, the condensation of volatiles would follow a similar sequence: oxygen/water first, when the temperature is higher, and carbon/organics later, when the temperature is lower. This would lead to deuterium fractions lower in water than in organics, regardless whether the synthesis of water and organic was on the gas phase or on the grain surfaces. Obviously, this is at the moment speculative but a road to explore, in our opinion. We emphasise that this “different epochs formation” hypothesis is fully compatible with the theory described in §9.2 of the origin of the organics deuteration from H₂D⁺ (Robert et al., 2011).

3. Why do most comets exhibit higher D/H water values, about a factor 2, than CCs and IDPs?

A possible answer is that comets are formed at distances, $\gtrsim 5$ AU, larger than those where the CCs originate, $\lesssim 4$ AU (Tab. 1; see also §9). A little more puzzling, though, is why the large majority of IDPs have D/H values lower than the cometary water, although at least 50% IDPs are predicted to be cometary fragments (Nesvorný et al. 2010). The new Herschel observations of JFC indicate indeed lower D/H values than those found in OCC (Tab. 3; §7), so that

the observed IDPs D/H values may be consistent with the cometary fragments theory. In conclusion, the D/H distribution of CCs and IDPs is a powerful diagnostic to probe the distribution of their origin in the PSN.

4. Why does the D/H distribution of the IDPs, which are thought to be fragments of comets, mimic the CCs bulk D/H distribution? And why is it asymmetric, namely with a shoulder towards the large D/H values?

As written above, the D/H ratio distribution depends on the distribution of the original distance from where CCs and IDPs come from or, in other words, their parental bodies. CCs are likely fragments of asteroids from the main belt and a good fraction is of cometary origin. IDPs are fragments from JFC and main belt asteroids. Their similar D/H distribution strongly suggests that the mixture of the two classes of objects is roughly similar, which argue for a difference between the two, more in terms of sizes than in origin. Besides, the asymmetric distribution testifies that a majority of CCs and IDPs originate from closer to the Sun parent bodies (see also Jacquet and Robert, 2013).

5. Why is the D/H ratio distribution of CC organics and

water so different?

There are in principle two possibilities: water and organics formed in different locations at the same time and then were mixed together or, on the contrary, they were formed at the same heliocentric distance but at (slightly) different epochs. The discussion in point 2 would favor the latter hypothesis, although this is speculative at the moment. If this is true, the D/H distribution potentially provides us with their history, namely when each of the two components formed. Again, being CC organics more D-enriched than water, they were formed at later stages.

10.2. Comparison between PPD and PSN models: need for a paradigm shift?

There are several differences between the Proto Planetary disks (PPDs) and Proto Solar Nebula (PSN) models. A first and major one is that PSN models assume a dense and hot phase for the solar PPD. For example, temperatures higher than 1000 K persist for $\sim 10^5$ yr at 3 AU and $\sim 10^6$ yr at 1 AU in the Yang et al. (2013) model. Generally, models of PPDs around Solar-type stars, on the contrary, never predict such high temperatures at those distances. Second, PPD models consider complex chemical networks with some horizontal and vertical turbulence which modifies, though not substantially, the chemical composition across the disk. On the contrary, in PSN models, chemistry networks are generally very simplified, whereas the turbulence plays a major role in the final D-enrichment across the disk. However, since the density adopted in the PSN models is very high, more complex chemical networks have a limited impact (Yang et al., 2013). Third, the above mentioned PSN models do not explicitly compute the dust particle coagulation and migration (if not as diffusion), and gas-grains decoupling whereas (some) disk models do (see Turner et al. and Testi et al., this volume).

In our opinion, the most significant difference is the first one and the urgent question to answer is: what is the good description of the PSN? A highly turbulent, hot and diffusive disk or a cooler and likely calmer disk, as the ones we see around T Tauri stars? Or something else?

The community of PSN models have reasons to think that the PSN disk was once hot. A major one is the measurement of depletion of moderately volatile elements (more volatile than silicon) in chondritic meteorites (Palme et al. 1988), which can be explained by dust coagulation during the cooling of an initially hot ($\gtrsim 1400$ K, the sublimation temperature of silicates) disk in the terrestrial planet formation region ($\lesssim 2$ AU; Lewis, 1974; Cameron and Truran, 1977; Cassen and Woolum, 1996). The explanation, though, assumes that the heating of the dust at $\gtrsim 1400$ K was global in extent, ordered and systematic. Alternatively, it is also possible that it was highly localised and, in this case, the hot initial nebula would be not necessary. For example, the so-called X-wind models assume that the hot processing occurs much closer to the star and then the matter is deposited outwards by the early Solar wind (Shu et al., 1996, 2000;

Gounelle et al., 2001). In addition, the detection of crystalline silicates in comets (Wooden et al., 2004) has been also taken as a prove that the Solar System passed through a hot phase (Mousis et al., 2007).

For sure, T Tau disks do not show the high temperatures ($\gtrsim 1400$ K at $r \sim 2$ AU) assumed by the PSN model. These temperatures are predicted in the midplane very close ($\lesssim 0.1$ AU) to the central star or in the high atmosphere of the disk, but always at distances lower than fractions of AU (Thi et al., 2010b). Even the most recent models of very young and embedded PPDs, with or without gravitational instabilities (see the review by Caselli and Ceccarelli, 2012), predict temperatures much lower than ~ 1400 K. One can ask whether the hot phase of the PSN could in fact be the hot corino phase observed in Class 0 sources (§5). Although the presently available facilities do not allow to probe regions of a few AUs, the very rough extrapolation of the temperature profile predicted for the envelope of IRAS16293-2422 (the prototype of Class 0 sources) by Crimier et al. (2010) gives ~ 1000 K at a few AUs. The question is, therefore: should we not compare the PSN with the hot corino models rather than the protoplanetary disks models? At present, the hot corino models are very much focused only on the $\gtrsim 10$ AU regions, which can be observationally probed, and only consider the gas composition. Should we not start, then, considering what happens in the very innermost regions of the Class 0 sources and study the dust fate too? If so, the link with the deuterium fractionation that we observe in the hot corino phase may become much more relevant in the construction of realistic PSN models. Last but not least, the present PSN models are based on the transport and mixing of material with different initial D/H water because of the diffusion, responsible for the angular momentum dispersion. In Class 0 sources, though, the dispersion of the angular momentum is thought to be mainly due to the powerful jets and outflows and not by the diffusion of inward/outward matter. Moreover, during the Class 0 phase, material from the cold protostellar envelope continues to rain down onto the central region and the accreting disk (Z.-Y. Li et al., this volume), replenishing them by highly deuterated material. The resulting D/H gradient across the PSN may, therefore, be different than that predicted by current theories.

10.3. Where does the terrestrial water come from?

Several reviews discussing the origin of the terrestrial water are present in the literature (Horner et al., 2009; Morbidelli et al., 2012; Caselli and Ceccarelli, 2012, van Dishoeck et al, this volume), so that we will here just summarise the points emphasising the open issues.

Let first remind that the water budget on Earth is itself subject of debate. In fact, while the lithosphere budget is relatively easy to measure ($\sim 10^{-4} M_{\oplus}$; Lécuyer et al., 1998), the water contained in the mantle, which contains by far the largest mass of our planet, is extremely difficult to measure and indirect probes, usually noble gases, are used

for that (e.g., *Allegre et al.*, 1983), with associated larger error bars. It is even more difficult to evaluate the water content of the early Earth, which was likely more volatile-rich than at present (*Kawamoto*, 1996). The most recent estimates give $\sim 2 \times 10^{-3} M_{\oplus}$ (*Marty*, 2012), namely 20 times larger than the value of the lithosphere water. If the water mantle is the dominant water reservoir, as it seems to be, then the D/H value of the terrestrial oceans may be misleading if geochemical processes can alter it. Evidently, measurements of the mantle water D/H is even more difficult. The last estimates suggest a value slightly lower than the terrestrial oceans water. In this chapter, given this uncertainty on the Earth bulk water content and D/H, we adopted as reference the evaporated ocean water D/H, the VSWOM (Tab. 1).

The “problem” of the origin of the terrestrial oceans rises because, if Earth was formed by planetesimals at ~ 1 AU heliocentric distance, they would have been “dry” and no water should exist on Earth. One theory, called “late veneer”, assumes that water was brought after Earth formed by, for example, comets (*Delsemme*, 1992; *Owen and Bar-Nun*, 1995). This theory is based on the assumptions that the D/H cometary water is the same than the Earth water D/H, but, based on observations towards comets (§7), this assumption is probably wrong. The second theory, based on the work by *Morbidelli et al.* (2000), assumes that a fraction of the planetesimals that built the Earth came from more distant (2–4 AU) regions and were, therefore, “wet”. Dynamical simulations of the early Solar System evolution have add support to this theory (*Morbidelli et al.*, 2000; *Morbidelli and Nesvorny*, 2012; *Raymond et al.*, 2009), challenging at the same time the idea that the flux of late veneer comets and asteroides could have been large enough to make up the amount of water on Earth. Moreover, the D/H value measured in CCs (§8) adds support to this theory. The recent findings by *Alexander et al.* would argue for a large contribution of a group of CCs, the CI type.

In summary, the origin of terrestrial water is still a source of intense debate.

11. SUMMARY AND FUTURE PROSPECTS

In this chapter we have established a link between the various phases in the process of Solar-type star and planet formation and our Solar System. This link has been metaphorically called the Ariadne’s thread and it is represented by the deuterium fractionation process. Deuterium fractionation is active everywhere in time and space, from pre-stellar cores, to protostellar envelopes and hot corinos, to protoplanetary disks. Its past activity can be witnessed by us today in comets, carbonaceous chondrites and interplanetary dust particles. Trying to understand and connect this process in the various phases of star and planet formation, while stretching the thread to our Solar System, has opened new horizons in the quest of our origins. The ultimate goal is to chemically and physically connect the various phases and identify the particular route taken by our Solar System.

The steps toward this goal are of course many, but much will be learned just starting with the following important points:

1. Bridge the gap between pre-stellar cores and protoplanetary disks and understand how different initial conditions affect the physical and chemical structure and evolution of protoplanetary disks.
2. Study the reprocessing of material during the early stages of protoplanetary disks; in particular, can self-gravitating accretion disks, thought to be in present in the hot corino/protostellar phase, help in understanding some of the observed chemical and physical features of more evolved protoplanetary disks and our Solar System?
3. Study the reprocessing of material (including dust coagulation and chemical evolution of trapped ices) throughout the protoplanetary disk evolution; in particular, which conditions do favour the production of the organic material observed in pristine bodies of our Solar-System?
4. Compare PSN models with protoplanetary disk models and include the main physical and chemical processes, in particular dust coagulation and ice mantle evolution.

The future is bright thanks to the great instruments available now and in the near future (e.g., ALMA and NOEMA, the ESA ROSETTA mission) and the advances in techniques used for the analysis of meteoritic material. Trying to fill the D/H plot shown in Fig.17 with new observations is of course one priority, but this needs to proceed hand in hand with developments in theoretical chemistry and more laboratory work. For sure, one lesson has been learned from this interdisciplinary work: our studies of the Solar System and our studies of star/planet forming regions represent two treasures which cannot be kept in two different coffers. It is now time to work together for a full exploitation of such treasures and eventually understand our astrochemical heritage.

Acknowledgments. C. Ceccarelli acknowledges the financial support from the French Agence Nationale pour la Recherche (ANR) (project FORCOMS, contract ANR-08-BLAN-0225) and the French spatial agency CNES. P. Caselli acknowledges the financial support of the European Research Council (ERC; project PALs 320620) and of successive rolling grants awarded by the UK Science and Technology Funding Council. O. Mousis acknowledges support from CNES. S. Pizzarello acknowledges support through the years from the NASA Exobiology and Origins of the Solar System Programs. D. Semenov acknowledges support by the *Deutsche Forschungsgemeinschaft* through SPP 1385: “The first ten million years of the solar system - a planetary materials approach” (SE 1962/1-1 and 1-2). This

research made use of NASA's Astrophysics Data System. We wish to thank A. Morbidelli, C. Alexander and L. Bonal for a critical reading of the manuscript. We also thank an anonymous referee and the Editor, whose comments helped to improve the chapter clarity.

REFERENCES

- Aikawa Y. and Nomura H. (2006) *Astrophys. J.*, 642, 1152.
 Akimkin V. et al. (2013) *Astrophys. J.*, 766, 8.
 Aléon J. et al. (2000) *Meteoritics and Planetary Science Supplement*, 35, 19.
 Alexander C. M. O. (2011) in: *IAU Symposium*, vol. 280 of *IAU Symposium*, (edited by J. Cernicharo and R. Bachiller), pp. 288–301.
 Alexander C. M. O. et al. (2012) *Science*, 337, 721.
 Allegre C. J. et al. (1983) *Nature*, 303, 762.
 Andrews S. M. and Williams J. P. (2007) *Astrophys. J.*, 659, 705.
 Andrews S. M. et al. (2009) *Astrophys. J.*, 700, 1502.
 Aresu G. et al. (2012) *Astron. Astrophys.*, 547, A69.
 Bacmann A. et al. (2002) *Astron. Astrophys.*, 389, L6.
 Bacmann A. et al. (2003) *Astrophys. J. Lett.*, 585, L55.
 Balsiger H. et al. (1995) *J. Geophys. Res.*, 100, 5827.
 Benson P. J. and Myers P. C. (1989) *Astrophys. J. Suppl.*, 71, 89.
 Bergin E. A. et al. (2013) *Nature*, 493, 644.
 Bitz S. M. C. and Nagy B. (1966) *Proceedings of the National Academy of Science*, 56, 1383.
 Biver N. et al. (2006) *Astron. Astrophys.*, 449, 1255.
 Bockelée-Morvan D. et al. (1998) *Icarus*, 133, 147.
 Bockelée-Morvan D. et al. (2012) *Astron. Astrophys.*, 544, L15.
 Bouwman J. et al. (2008) *Astrophys. J.*, 683, 479.
 Brassier R. (2008) *Astron. Astrophys.*, 492, 251.
 Brassier R. and Morbidelli A. (2013) *Icarus*, 225, 40.
 Brown R. H. et al. (2012) *Planet. Space Sci.*, 60, 166.
 Butner H. M. et al. (1995) *Astrophys. J.*, 448, 207.
 Butner H. M. et al. (2007) *Astrophys. J. Lett.*, 659, L137.
 Callahan M. P. et al. (2011) *Proceedings of the National Academy of Science*, 108, 13995.
 Cameron A. G. W. and Truran J. W. (1977) *Icarus*, 30, 447.
 Caselli P. and Ceccarelli C. (2012) *Astron. Astrophys. Rev.*, 20, 56.
 Caselli P. et al. (1999) *Astrophys. J. Lett.*, 523, L165.
 Caselli P. et al. (2002) *Astrophys. J.*, 565, 344.
 Caselli P. et al. (2003) *Astron. Astrophys.*, 403, L37.
 Caselli P. et al. (2008) *Astron. Astrophys.*, 492, 703.
 Caselli P. et al. (2012) *Astrophys. J. Lett.*, 759, L37.
 Cassen P. and Woolum D. S. (1996) *Astrophys. J.*, 472, 789.
 Cazaux S. et al. (2011) *Astrophys. J. Lett.*, 741, L34.
 Ceccarelli C. and Dominik C. (2005) *Astron. Astrophys.*, 440, 583.
 Ceccarelli C. et al. (1996) *Astrophys. J.*, 471, 400.
 Ceccarelli C. et al. (1998) *Astron. Astrophys.*, 338, L43.
 Ceccarelli C. et al. (2000) *Astron. Astrophys.*, 357, L9.
 Ceccarelli C. et al. (2007) *Protostars and Planets V*, pp. 47–62.
 Charnley S. B. et al. (1997) *Astrophys. J. Lett.*, 482, L203.
 Cleeves L. I. et al. (2011) *Astrophys. J. Lett.*, 743, L2.
 Codella C. et al. (2010) *Astron. Astrophys.*, 522, L1.
 Codella C. et al. (2012) *Astrophys. J. Lett.*, 757, L9.
 Cody G. D. and Alexander C. M. O. (2005) *Geochim. Cosmochim. Acta*, 69, 1085.
 Cody G. D. et al. (2011) *Proceedings of the National Academy of Science*, 108, 19171.
 Coutens A. et al. (2012) *Astron. Astrophys.*, 539, A132.
 Coutens A. et al. (2013a) *Astron. Astrophys.*, 560, A39.
 Coutens A. et al. (2013b) *Astron. Astrophys.*, 553, A75.
 Crapsi A. et al. (2005) *Astrophys. J.*, 619, 379.
 Crapsi A. et al. (2007) *Astron. Astrophys.*, 470, 221.
 Crimier N. et al. (2010) *Astron. Astrophys.*, 519, A65.
 Crovisier J. et al. (2004) *Astron. Astrophys.*, 418, 1141.
 Czaja A. D. (2010) *Nature Geoscience*, 3, 522.
 Dalgarno A. and Lepp S. (1984) *Astrophys. J. Lett.*, 287, L47.
 Dartois E. et al. (2003) *Astron. Astrophys.*, 399, 1009.
 Deloule E. et al. (1998) *Geochim. Cosmochim. Acta*, 62, 3367.
 Delsemme A. H. (1992) *Advances in Space Research*, 12, 5.
 Derenne S. and Robert F. (2010) *Meteoritics and Planetary Science*, 45, 1461.
 Dominik C. et al. (2005) *Astrophys. J. Lett.*, 635, L85.
 Dones L. et al. (2004) *Oort cloud formation and dynamics*, pp. 153–174.
 Drouart A. et al. (1999) *Icarus*, 140, 129.
 Dulieu F. et al. (2010) *Astron. Astrophys.*, 512, A30.
 Dullemond C. P. et al. (2002) *Astron. Astrophys.*, 389, 464.
 Duncan M. J. and Levison H. F. (1997) *Science*, 276, 1670.
 Eberhardt P. et al. (1995) *Astron. Astrophys.*, 302, 301.
 Elsilá J. E. et al. (2012) *Meteoritics and Planetary Science*.
 Evans II N. J. et al. (2009) *Astrophys. J. Suppl.*, 181, 321.
 Flower D. R. et al. (2006) *Astron. Astrophys.*, 449, 621.
 Fogel J. K. J. et al. (2011) *Astrophys. J.*, 726, 29.
 Friesen R. K. et al. (2013) *Astrophys. J.*, 765, 59.
 Gálvez Ó. et al. (2011) *Astrophys. J.*, 738, 133.
 Garrod R. et al. (2006) *Faraday Discussions*, 133, 51.
 Geiss J. and Gloeckler G. (1998) *Space Sci. Rev.*, 84, 239.
 Geiss J. and Reeves H. (1981) *Astron. Astrophys.*, 93, 189.
 Gerlich D. and Schlemmer S. (2002) *Planet. Space Sci.*, 50, 1287.
 Gibb E. L. et al. (2012) *Astrophys. J.*, 750, 102.
 Gounelle M. et al. (2001) *Astrophys. J.*, 548, 1051.
 Gourier D. et al. (2008) *Geochim. Cosmochim. Acta*, 72, 1914.
 Grady C. A. et al. (2013) *Astrophys. J.*, 762, 48.
 Guilloteau S. et al. (2006) *Astron. Astrophys.*, 448, L5.
 Guilloteau S. et al. (2011) *Astron. Astrophys.*, 529, A105.
 Hartogh P. et al. (2011) *Nature*, 478, 218.
 Henning T. and Semenov D. (2013) *Chemical Reviews*, 113, 9016.
 Henning T. et al. (2010) *Astrophys. J.*, 714, 1511.
 Hersant F. et al. (2001) *Astrophys. J.*, 554, 391.
 Hiraoka K. et al. (1998) *Astrophys. J.*, 498, 710.
 Hirota T. et al. (2003) *Astrophys. J.*, 594, 859.
 Hollenbach D. et al. (2009) *Astrophys. J.*, 690, 1497.
 Horner J. et al. (2007) *Earth Moon and Planets*, 100, 43.
 Horner J. et al. (2008) *Planet. Space Sci.*, 56, 1585.
 Horner J. et al. (2009) *Planet. Space Sci.*, 57, 1338.
 Hutsemékers D. et al. (2008) *Astron. Astrophys.*, 490, L31.
 Ilee J. D. et al. (2011) *Mon. Not. R. Astron. Soc.*, 417, 2950.
 Jaquet E. and Robert F. (2013) *Icarus*, 223, 722.
 Jehin E. et al. (2009) *Earth Moon and Planets*, 105, 167.
 Jørgensen J. K. and van Dishoeck E. F. (2010) *Astrophys. J. Lett.*, 725, L172.
 Jørgensen J. K. et al. (2002) *Astron. Astrophys.*, 389, 908.
 Kavelaars J. J. et al. (2011) *Astrophys. J. Lett.*, 734, L30.
 Kawamoto T. (1996) *Earth and Planetary Science Letters*, 144, 577.
 Keto E. and Caselli P. (2008) *Astrophys. J.*, 683, 238.
 Keto E. and Caselli P. (2010) *Mon. Not. R. Astron. Soc.*, 402, 1625.
 Kwok S. (2004) *Nature*, 430, 985.
 Lécluse C. and Robert F. (1994) *Geochim. Cosmochim. Acta*, 58, 2927.

- Lécuyer C. et al. (1998) *Chemical Geology*, 145, 249.
- Lee C. W. and Myers P. C. (2011) *Astrophys. J.*, 734, 60.
- Levison H. F. et al. (2008) *Icarus*, 196, 258.
- Levison H. F. et al. (2010) *Science*, 329, 187.
- Lewis J. S. (1974) *Science*, 186, 440.
- Li D. and Goldsmith P. F. (2003) *Astrophys. J.*, 585, 823.
- Linsky J. L. (2007) *Space Sci. Rev.*, 130, 367.
- Lis D. C. et al. (2002) *Astrophys. J. Lett.*, 571, L55.
- Lis D. C. et al. (2013) *Astrophys. J. Lett.*, 774, L3.
- Liu F.-C. et al. (2011) *Astron. Astrophys.*, 527, A19.
- Loiuard L. et al. (2001) *Astrophys. J. Lett.*, 552, L163.
- Lubowich D. A. et al. (2000) *Nature*, 405, 1025.
- Marcelino N. et al. (2005) *Astrophys. J.*, 620, 308.
- Maret S. et al. (2004) *Astron. Astrophys.*, 416, 577.
- Maret S. et al. (2005) *Astron. Astrophys.*, 442, 527.
- Marty B. (2012) *Earth and Planetary Science Letters*, 313, 56.
- Mathews G. S. et al. (2013) *ArXiv e-prints*.
- Maury A. J. et al. (2010) *Astron. Astrophys.*, 512, A40.
- McKee C. F. and Ostriker E. C. (2007) *Annu. Rev. Astron. Astrophys.*, 45, 565.
- Meier R. et al. (1998a) *Science*.
- Meier R. et al. (1998b) *Science*.
- Messenger S. (2000) *Nature*, 404, 968.
- Morbidelli A. and Nesvorný D. (2012) *Astron. Astrophys.*, 546, A18.
- Morbidelli A. et al. (2000) *Meteoritics and Planetary Science*, 35, 1309.
- Morbidelli A. et al. (2012) *Annual Review of Earth and Planetary Sciences*, 40, 251.
- Mousis O. (2004) *Astron. Astrophys.*, 414, 1165.
- Mousis O. et al. (2000) *Icarus*, 148, 513.
- Mousis O. et al. (2007) *Astron. Astrophys.*, 466, L9.
- Nagaoka A. et al. (2005) *Astrophys. J. Lett.*, 624, L29.
- Nesvorný D. et al. (2010) *Astrophys. J.*, 713, 816.
- Nomura H. et al. (2007) *Astrophys. J.*, 661, 334.
- Oba Y. et al. (2012) *Astrophys. J.*, 749, 67.
- Öberg K. I. et al. (2012) *Astrophys. J.*, 749, 162.
- Owen T. and Bar-Nun A. (1995) *Icarus*, 116, 215.
- Pagani L. et al. (2007) *Astron. Astrophys.*, 467, 179.
- Parise B. et al. (2002) *Astron. Astrophys.*, 393, L49.
- Parise B. et al. (2003) *Astron. Astrophys.*, 410, 897.
- Parise B. et al. (2004) *Astron. Astrophys.*, 416, 159.
- Parise B. et al. (2006) *Astron. Astrophys.*, 453, 949.
- Parise B. et al. (2011) *Astron. Astrophys.*, 526, A31.
- Peltzer E. T. and Bada J. L. (1978) *Nature*, 272, 443.
- Persson M. V. et al. (2012) *Astron. Astrophys.*, 541, A39.
- Pizzarello S. and Groy T. L. (2011) *Geochim. Cosmochim. Acta*, 75, 645.
- Pizzarello S. and Huang Y. (2005) *Geochim. Cosmochim. Acta*, 69, 599.
- Pizzarello S. et al. (2004) *Geochim. Cosmochim. Acta*, 68, 4963.
- Pizzarello S. et al. (2006) *The Nature and Distribution of the Organic Material in Carbonaceous Chondrites and Interplanetary Dust Particles*, pp. 625–651.
- Pizzarello S. et al. (2012) *Proceedings of the National Academy of Science*, 109, 11949.
- Qi C. et al. (2008a) *Astrophys. J.*, 681, 1396.
- Qi C. et al. (2008b) *Astrophys. J.*, 681, 1396.
- Qi C. et al. (2013) *ArXiv e-prints*.
- Ratajczak A. et al. (2009) *Astron. Astrophys.*, 496, L21.
- Ratajczak A. et al. (2011) *Astron. Astrophys.*, 528, L13.
- Raymond S. N. et al. (2009) *Icarus*, 203, 644.
- Remusat L. et al. (2005) in: vol. 36 of *Lunar and Planetary Institute Science Conference Abstracts*, (edited by S. Mackwell and E. Stansbery), p. 1350.
- Remusat L. et al. (2006) *Earth and Planetary Science Letters*, 243, 15.
- Remusat L. et al. (2009) *Astrophys. J.*, 698, 2087.
- Remusat L. et al. (2012) *Geochim. Cosmochim. Acta*, 96, 319.
- Richet P. et al. (1977) *Annual Review of Earth and Planetary Sciences*, 5, 65.
- Rist C. et al. (2013) *Journal of Physical Chemistry A*, 117, 9800.
- Robert F. and Derenne S. (2006) *Meteoritics and Planetary Science Supplement*, 41, 5259.
- Robert F. and Epstein S. (1982) *Geochim. Cosmochim. Acta*, 46, 81.
- Robert F. et al. (1979) *Nature*, 282, 785.
- Robert F. et al. (2011) *Geochim. Cosmochim. Acta*, 75, 7522.
- Roberts H. and Millar T. J. (2000) *Astron. Astrophys.*, 361, 388.
- Roberts H. et al. (2003) *Astrophys. J. Lett.*, 591, L41.
- Roueff E. et al. (2005) *Astron. Astrophys.*, 438, 585.
- Schmitt-Kopplin P. et al. (2010) *Proceedings of the National Academy of Science*, 107, 2763.
- Shah R. Y. and Wootten A. (2001) *Astrophys. J.*, 554, 933.
- Shu F. H. et al. (1996) *Science*, 271, 1545.
- Shu F. H. et al. (2000) *Protostars and Planets IV*, p. 789.
- Sipilä O. et al. (2013) *Astron. Astrophys.*, 554, A92.
- Spezzano S. et al. (2013) *Astrophys. J. Lett.*, 769, L19.
- Taquet V. et al. (2012a) *Astrophys. J. Lett.*, 748, L3.
- Taquet V. et al. (2012b) *Astron. Astrophys.*, 538, A42.
- Taquet V. et al. (2013a) *Astrophys. J. Lett.*, 768, L29.
- Taquet V. et al. (2013b) *Astron. Astrophys.*, 550, A127.
- Thi W.-F. et al. (2010a) *Astron. Astrophys.*, 518, L125.
- Thi W.-F. et al. (2010b) *Mon. Not. R. Astron. Soc.*, 407, 232.
- Turner B. E. (2001) *Astrophys. J. Suppl.*, 136, 579.
- van der Tak F. F. S. et al. (2002) *Astron. Astrophys.*, 388, L53.
- van Dishoeck E. F. et al. (2003) *Astron. Astrophys.*, 400, L1.
- Vastel C. et al. (2003) *Astrophys. J. Lett.*, 593, L97.
- Vastel C. et al. (2004) *Astrophys. J. Lett.*, 606, L127.
- Vastel C. et al. (2010) *Astron. Astrophys.*, 521, L31.
- Vasyunin A. I. et al. (2011) *Astrophys. J.*, 727, 76.
- Villanueva G. L. et al. (2009) *Astrophys. J. Lett.*, 690, L5.
- Visser R. et al. (2013) *Astrophys. J.*, 769, 19.
- Waite Jr. J. H. et al. (2009) *Nature*, 460, 487.
- Walmsley C. M. et al. (2004) *Astron. Astrophys.*, 418, 1035.
- Walsh K. J. et al. (2011) *Nature*, 475, 206.
- Ward-Thompson D. et al. (1999) *Mon. Not. R. Astron. Soc.*, 305, 143.
- Weaver H. A. et al. (2008) *LPI Contributions*, 1405, 8216.
- Weber A. S. et al. (2009) *Astrophys. J.*, 703, 1030.
- Whittet D. C. B. et al. (2007) *Astrophys. J.*, 655, 332.
- Willacy K. (2007) *Astrophys. J.*, 660, 441.
- Willacy K. and Woods P. M. (2009) *Astrophys. J.*, 703, 479.
- Williams J. P. and Cieza L. A. (2011) *Ann. Rev. Astron. Astrophys.*, 49, 67.
- Woitke P. et al. (2009) *Astron. Astrophys.*, 501, 383.
- Wooden D. H. et al. (2004) *Astrophys. J. Lett.*, 612, L77.
- Yang J. and Epstein S. (1983) *Geochim. Cosmochim. Acta*, 47, 2199.
- Yang L. et al. (2013) *Icarus*.
- Zinner E. et al. (1983) *Nature*, 305, 119.